two functionally different human progesterone receptor forms A and B. *EMBO J.* **9**, 1603–1614.

Katsuyama, M., Ikegami, R., Karahashi, H., Amano, F., Sugimoto, Y. & Ichikawa, A. (1998a) Characterization of the LPS-stimulated expression of EP2 and EP4 prostaglandin E receptors in mouse macrophage-like cell line, J774.1. *Biochem. Biophys. Res. Commun.* **251**, 727–731.

Katsuyama, M., Nishigaki, N., Sugimoto, Y., *et al.* (1995) The mouse prostaglandin E receptor EP_2 subtype: cloning, expression, and Northern blot analysis. *FEBS Lett.* **372**, 151–156.

Katsuyama, M., Sugimoto, Y., Morimoto, K., *et al.* (1997) Distinct cellular localization of the messenger ribonucleic acid for prostaglandin E receptor subtypes in the mouse uterus during pseudopregnancy. *Endocrinology* **138**, 344–350.

Katsuyama, M., Sugimoto, Y., Okano, K., *et al.* (1998b) Characterization of the gene for the mouse prostaglandin E receptor subtype EP_2: tissue-specific initiation of transcription in the macrophage and the uterus. *Biochem. J.* **330**, 1115–1121.

Kennedy, T.G., Martel, D. & Psychoyos, A. (1983) Endometrial prostaglandin E_2 binding during the estrous cycle and its hormonal control in ovariectomized rats. *Biol. Reprod.* **29**, 565–571.

Kepa, J.K., Jacobsen, B.M., Boen, E.A., *et al.* (1996) Direct binding of progesterone receptor to nonconsensus DNA sequences represses rat GnRH. *Mol. Cell. Endocrinol.* **117**, 27–39.

Lamian, V., Gonzalez, B.Y., Michel, F.J. & Simmen, R.C.M. (1993) Non-consensus progesterone response elements mediate the progesterone-regulated endometrial expression of the uteroferrin gene. *J. Steroid Biochem. Mol. Biol.* **46**, 439–450.

LeVan, T.D., Bloom, J.W., Bailey, T.J., *et al.* (2001) A common single nucleotide polymorphism in the CD14 promoter decreases the affinity of Sp protein binding and enhances transcriptional activity. *J. Immunol.* **167**, 5838–5844.

Lim, H. & Dey, S.K. (1997) Prostaglandin E_2 receptor subtype EP_2 gene expression in the mouse uterus coincides with differentiation of the luminal epithelium for implantation. *Endocrinology* **138**, 4599–4606.

Owen, G.I., Richer, J.K., Tung, L., Takimoto, G. & Horwitz, K.B. (1998) Progesterone regulates transcription of the $p21^{WAF1}$ cyclindependent kinase inhibitor gene through Sp1 and CBP/p300. *J. Biol. Chem.* **273**, 10696–10701.

Regan, J.W., Bailey, T.J., Pepperl, D.J., *et al.* (1994) Cloning of a novel human prostaglandin receptor with characteristics of the pharmacologically defined EP_2 subtype. *Mol. Pharmacol.* **46**, 213–220.

Schott, D.R., Shyamala, G., Schneider, W. & Parry, G. (1991) Molecular cloning, sequence analyses, and expression of complementary DNA encoding murine progesterone receptor. *Biochemistry* **30**, 7014–7020.

Segi, E., Haraguchi, K., Sugimoto, Y., *et al.* (2003) Expression of messenger RNA for prostaglandin E receptor subtypes EP4/EP2 and cyclooxygenase isozymes in mouse periovulatory follicles and oviducts during superovulation. *Biol. Reprod.* **68**, 804–811.

Shou, Y., Baron, S. & Poncz, M. (1998) An Sp1-binding silencer element is a critical negative regulator of the megakaryocyte-specific α_{IIb} gene. *J. Biol. Chem.* **273**, 5716–5726.

Skak, K. & Michelsen, B.K. (1999) The TATA-less rat GAD65 promoter can be activated by Sp1 through non-consensus elements. *Gene* **236**, 231–241.

Smock, S.L., Pan, L.C., Castleberry, T.A., Lu, B., Mather, R.J. & Owen, T.A. (1999) Cloning, structural characterization, and chromosomal localization of the gene encoding the human prostaglandin E_2 receptor EP2 subtype. *Gene* **237**, 393–402.

Sonoshita, M., Takaku, K., Sasaki, N., *et al.* (2001) Acceleration of intestinal polyposis through prostaglandin receptor EP2 in $Apc^{\Delta 716}$ knockout mice. *Nature Med.* **7**, 1048–1051.

Stoner, M., Wang, F., Wormke, M., *et al.* (2000) Inhibition of vascular endothelial growth factor expression in HEC1A endometrial cancer cells through interactions of estrogen receptor α and Sp3 proteins. *J. Biol. Chem.* **275**, 22769–22779.

Sugimoto, Y., Narumiya, S. & Ichikawa, A. (2000) Distribution and function of prostanoid receptors: studies from knockout mice. *Prog. Lipid Res.* **39**, 289–314.

Tang, M., Mazella, J., Gao, J. & Tseng, L. (2002) Progesterone receptor activates its promoter activity in human endometrial stromal cells. *Mol. Cell. Endocrinol.* **192**, 45–53.

Thomson, A.A., Ham, J., Bakker, O. & Parker, M.G. (1990) The progesterone receptor can regulate transcription in the absence of a functional TATA box element. *J. Biol. Chem.* **265**, 16709–16712.

Wen, D.X., Xu, Y.F., Mais, D.E., Goldman, M.E. & McDonnell, D.P. (1994) The A and B isoforms of the human progesterone receptor operate through distinct signaling pathways within target cells. *Mol. Cell. Biol.* **14**, 8356–8364.

Xu, Q., Ji, Y.S. & Schmedtje, J.F. Jr (2000) Sp1 increases expression of cyclooxygenase-2 in hypoxic vascular endothelium. *J. Biol. Chem.* **275**, 24583–24589.

Received: 6 February 2003
Accepted: 14 June 2003

Inflamm. res. 52, *Supplement 1* (2003) S59–S62
1023-3830/03/01S59-04

Inflammation Research

Phosphorothioate antisense oligodeoxynucleotides against histidine decarboxylase: a study in mouse mammary epithelial cell cultures

W. Wagner[1], S. Tanaka[2], A. Ichikawa[2] and W A. Fogel[1]

[1] Institute of Biogenic Amines, Polish Academy of Sciences, Tylna 3, 90-364 Lodz, Poland, Fax: ++ 48 42 6815283, e-mail: waldemaw@amina1.zabpan.lodz.pl

[2] Department of Physiological Chemistry, Faculty of Pharmaceutical Sciences, Kyoto University, Sakyo-ku, Kyoto 606, Japan

Introduction

Physiological changes in expression of histidine decarboxylase (HDC) and presence of histamine in mouse mammary epithelial cells have been described recently [6]. Glandular histamine in normal mammary cells and in mammary carcinomas is regarded as an important auto- and paracrine growth factor acting through H_1 and H_2 histaminergic receptors [2, 6, 7]. Coexistence of histamine producing epithelial cells and mastocytes, plus distribution of H_1, H_2 and H_3 receptors in mammary tissue emphasizes its importance in mammary development and function. In this study, we have developed potent phosphorothioate antisense oligodeoxynucleotides against HDC to confirm the physiological relevance of histamine synthesis in mammary gland.

Materials and methods

Antisense phosphorothioate oligodeoxynucleotides ([S]ODNs) were designed to target mouse HDC mRNA (Accession X57437): HDC0062 (cDNA: nt 62–90), HDC0097 (cDNA: nt 97–115), HDC0578 (cDNA: nt 578–596), HDC1085 (cDNA: nt 1085–1102), HDC1253 (cDNA: nt 1253–1268) and HDC1940 (cDNA: nt 1940–1959). All [S]ODNs, except for HDC1253 [4] were our own design. The computational simulation using mfold 3.1 software (by Zuker and Turner) [8] was applied. HDC0062S and HDC1253S (sense oligonucleotides) and HDC1085 sequence in random order (HDC1085RD) were used as specificity controls.

In vitro [S]ODNs exposure

Primary mammary epithelial cell cultures were prepared and cultured as described [6]. Epithelial organoids (300–400/well) were seeded on 24-well plates and incubated for 24 h prior to start of experiment. Antisense, sense or scrambled [S]ODNs (0.5–10 μM) were applied to 24 h and 72 h cultures with fresh medium change.

Correspondence to: W. Wagner

HDC and histamine assays

48 h after second [S]ODNs treatment, cells and medium were harvested. HDC activity was estimated using method of Taguchi et al. [5] except, newly synthesised histamine was measured by radioenzymatic assay [3]. Postculture medium harvested 48 h after each [S]ODNs treatment was deproteinized and total histamine content was measured [3].

Immunocytochemistry

For HDC immunostaining [1] primary cell culture growing on 8-chamber glass slides were used. [S]ODNs treatments were as described above.

Data analysis

Data are presented as mean ± SEM. Comparisons between groups were carried out using analysis of variance (ANOVA) and Newman-Keuls *post hoc* test.

Results and discussion

Out of six antisense [S]ODNs initially tested at 1, 5 and 10 μM only HDC0062, HDC1253 and HDC1085 exerted dose-response significant antisense effects as compared to control [S]ODNs untreated group (Fig. 1, Experiment I). There was some unexpected HDC inhibition by HDC1085RD and it was associated with 96 h/48 h histamine index variation (80%, 126% and 88% of untreated group for 1, 5 and 10 μM, respectively; data not shown).

The most efficient HDC0062 and HDC1253 were further tested at concentrations of 0.5–10 μM. HDC0062 was found to inhibit HDC specifically at concentrations of 0.5 and 5–10 μM (Fig. 1, Experiment II). Some nonspecific action of sense [S]ODNs was seen at 1 and 2.5 μM. Thus slight decrease of histamine medium content was found at 0.5, 1, 2.5 and 5 μM and calculated 96 h/48 h histamine index were 95%, 53%, 64% and 90%, respectively compared to respective sense [S]ODNs (data not shown). Immunocytochemical evidence indicated down-regulation of HDC expression by

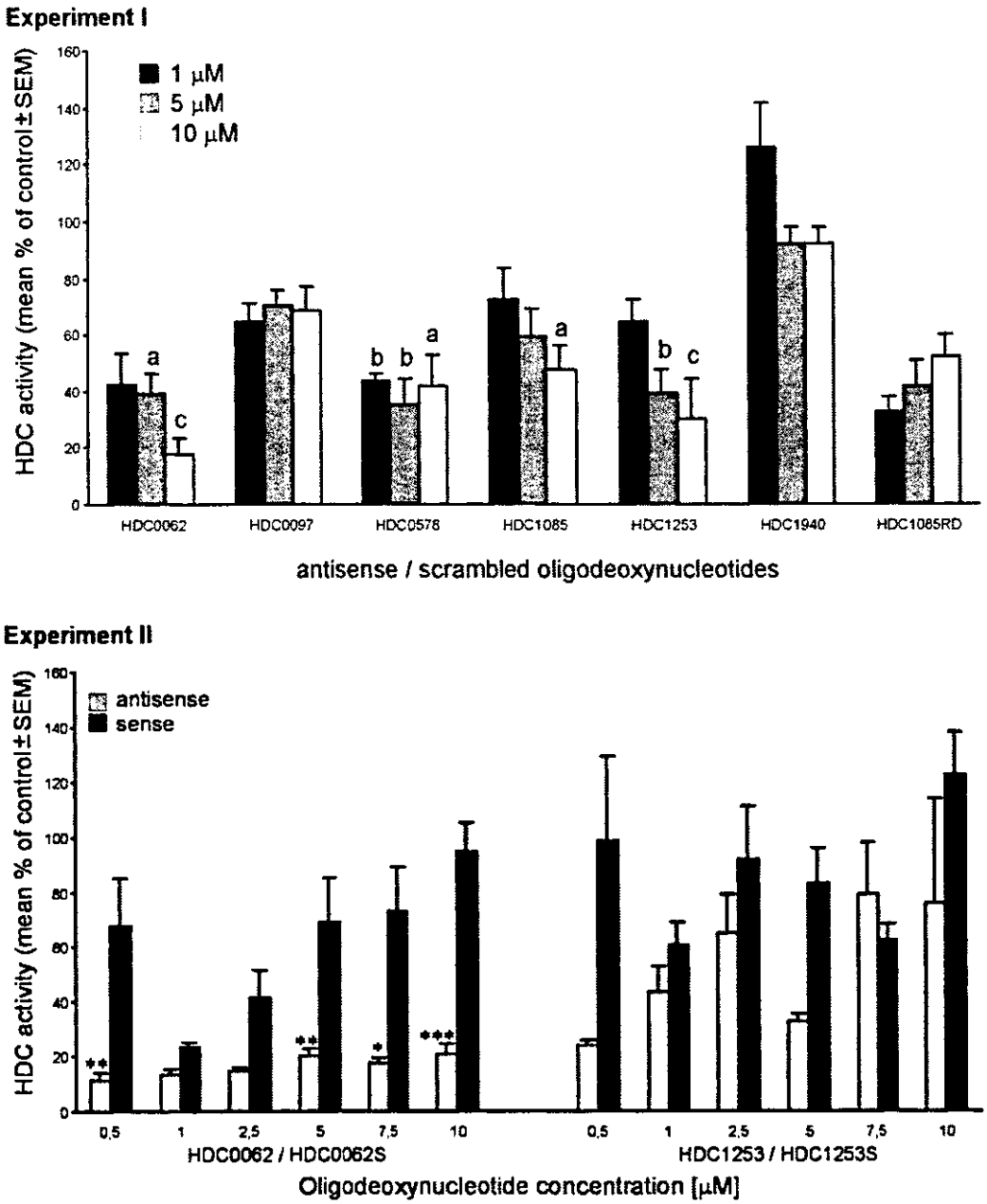

Fig. 1. HDC activity levels following treatment with different doses of antisense, sense and scrambled [S]ODNs. Values represent the mean % ± SEM (n = 3–5), relative to that obtained in control cultures not exposed to any [S]ODNs.Experiment I-first experiment, Experiment II-second experiment. $^{a}p < 0.05$, $^{b}p < 0.01$, $^{c}p < 0.001$ vs control; $*p < 0.05$, $**p < 0.01$, $***p < 0.001$ vs respective sense [S]ODNs (Newman-Keuls test).

HDC0062, even at concentrations of 0.1 and 0.5 µM (Fig. 2). Evidence for HDC inhibition by HDC1253 was less clear. Although, immunocytochemical study showed inhibition of cell HDC expression by HDC1253 at 1, 5 and 10 µM (data not shown), decrease in enzyme activity could be seen mostly at 0.5 and 5 µM (Fig. 1, Experiment II).

Experiments reported here demonstrated the successful decrement of HDC expression by application of thioated antisense oligodeoxynucleotides for HDC in mammary epithelial primary cell culture. Efficient targeting of HDC translation in vitro by HDC0062 oligonucleotide suggests phosphorothioate-modified antisense ODNs are good tools for studying histamine's function in mammary gland. Future work will look at use of HDC oligonucleotides in vivo.

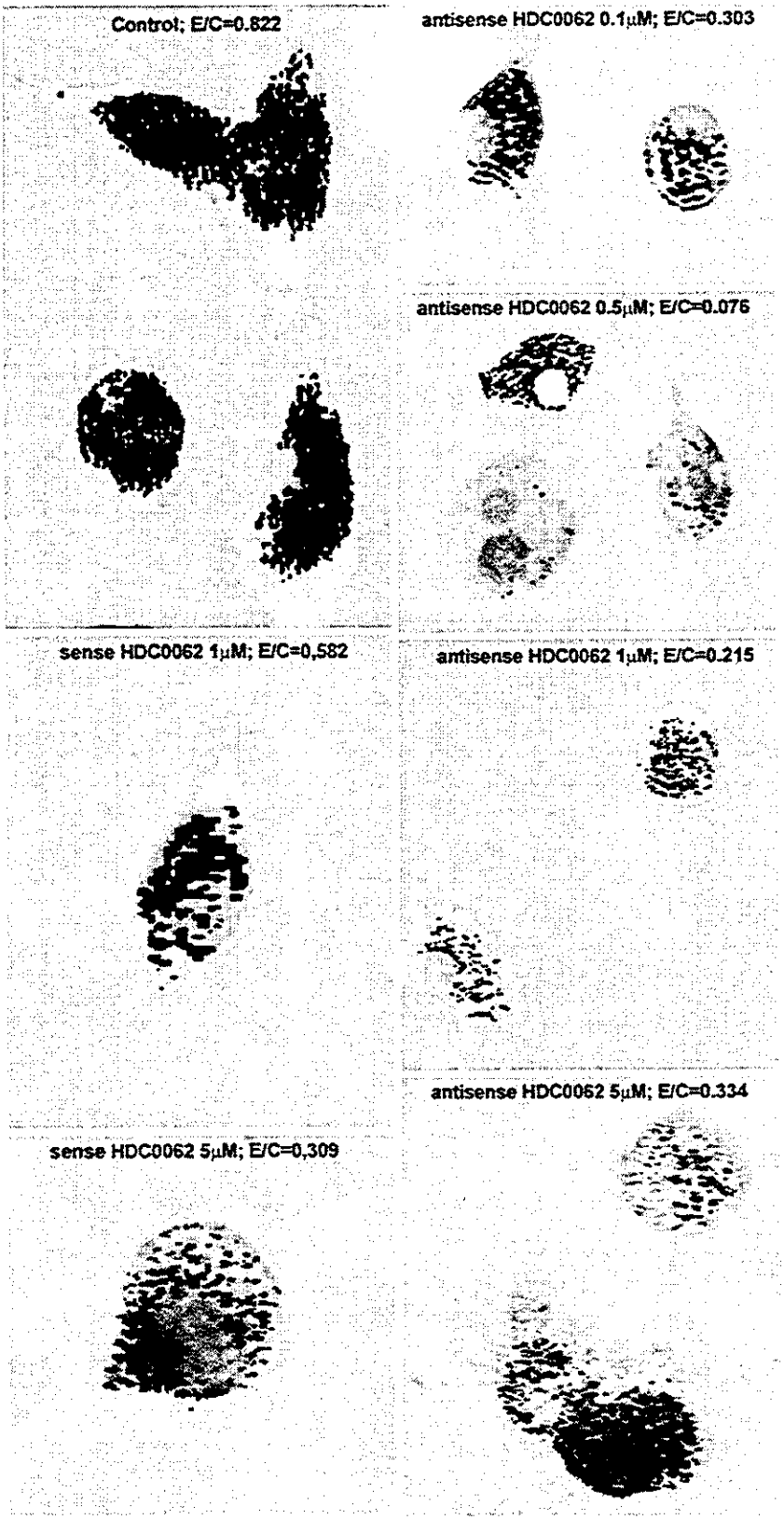

Fig. 2. Effects of HDC0062/HDC0062S on HDC expression of mammary epithelial cells. E/C index is the enzyme expression area (black)/cytoplasmic area (gray).

References

[1] Asahara M, Mushiake S, Shimada S, Fukui H, Kinoshita Y, Kawanami C et al. Reg gene expression is increased in rat gastric enterochromaffin-like cells following water immersion stress. Gastroenterology 1996; 111: 45–55.

[2] Cricco GP, Davio CA, Martin G, Engel N, Fitzsimons CP, Bergoc R et al. Histamine as an autocrine growth factor in experimental mammary carcinomas. Agents Actions 1994; 43.

[3] Fogel WA, Andrzejewski W, Maslinski C. Brain histamine in rats with hepatic encephalopathy. J Neurochem 1991; 56: 38–43

[4] Hegyesi H, Somlai B, Lia Varga V, Toth G, Kovacs P, Molnar EL et al. Suppression of melanoma cell proliferation by histidine decarboxylase specific antisense oligonucleotides. J Invest Dermatol 2001; 117: 151–3.

[5] Taguchi Y, Watanabe T, Kubota H, Hayashi H, Wada H. Purification of histidine decarboxylase from the liver of fetal rats and its immunochemical and immunohistochemical characterization. J Biol Chem 1984; 259: 5214–21.

[6] Wagner W, Kobos J, Fogel WA. Histamine synthesis by mouse mammary gland epithelial cells in primary culture. The effects of mammary gland differentation stage (pregnancy, lactation). Inflamm res Suppl. 2 2001; 50: S104–5.

[7] Wagner W, Stasiak A, Fogel WA. Mouse mammary epithelial cells bear histamine receptors. Inflamm Res Suppl. 1 2002; 51: S81–2.

[8] Zuker M, Mathews DH, Turner DH. Algorithms and Thermodynamics for RNA Secondary Structure Prediction: A Practical Guide. In Barciszewski J, Clark BFC, eds. RNA Biochemistry and Biotechnology. NATO ASI Series, Kluwer Academic Publishers, 1999:11–43.

Available online at www.sciencedirect.com
SCIENCE DIRECT®
Biochemical and Biophysical Research Communications 322 (2004) 911–917
BBRC
www.elsevier.com/locate/ybbrc

Microarray evaluation of EP4 receptor-mediated prostaglandin E_2 suppression of 3T3-L1 adipocyte differentiation

Yukihiko Sugimoto[a,1], Hiroaki Tsuboi[a,1], Yasushi Okuno[b], Shigero Tamba[a], Soken Tsuchiya[a], Gozo Tsujimoto[b], Atsushi Ichikawa[a,c,*]

[a] *Department of Physiological Chemistry, Kyoto University Graduate School of Pharmaceutical Sciences, Sakyo-ku, Kyoto 606-8501, Japan*
[b] *Department of Genomic Drug Discovery Science, Kyoto University Graduate School of Pharmaceutical Sciences, Sakyo-ku, Kyoto 606-8501, Japan*
[c] *School of Pharmaceutical Sciences, Mukogawa Women's University, Koshien, Nishinomiya, Hyogo 663-8179, Japan*

Received 22 June 2004

Abstract

Prostaglandin E_2 (PGE_2) has been shown to negatively regulate adipogenesis. To explore to what extent PGE_2 inhibits the differentiation of cells to adipocytes and to examine whether its effect could be due to EP4 receptor signaling, we used microarrays to analyze the gene expression profiles of 3T3-L1 cells exposed to a differentiation cocktail supplemented with PGE_2, AE1-329 (an EP4 agonist), or vehicle. The differentiation-associated responses in genes such as adipocytokines and enzymes related to lipid metabolism were largely weakened upon PGE_2 treatment. In particular, the expression of peroxisome proliferator activated receptor-γ and CCAAT/enhancer binding protein-α, genes playing a central role in adipogenesis, was greatly suppressed. PGE_2 appears to be ineffective to a subclass of insulin target genes such as hexokinase 2 and phosphofructokinase. Similar responses were produced in the differentiation-associated genes upon AE1-329 treatment. These results suggest that PGE_2 inhibits a crucial step of the adipocyte differentiation process by acting on the EP4 receptor in 3T3-L1 cells.

Keywords: Prostanoid; Receptor subtype; Fat cell; Aspirin-like drugs; Gene expression profile

Adipogenesis is a crucial aspect in controlling body fat mass [1,2]. Acquisition of the mature adipocyte phenotype is a highly regulated process in which preadipocytes undergo differentiation resulting in both increased size and number of mature adipocytes in the adipose tissue. It has been shown that cyclooxygenase (COX) products such as prostaglandin (PG) E_2 and $PGF_{2\alpha}$ inhibit adipocyte development [3–7]. A recent study suggested that COX-2 might be involved in body fat regulation [8]. Mice heterozygous for the COX-2 gene showed increased body weight by about 30%, with fat pads enlarged 2- to 3-fold compared with those of wild-type animals. PGE_2 production in adipose tissue from COX-2 null mice was only 20% of that of wild-type mice. These results suggested that COX-2 as well as PGE_2 participates in the negative regulation of adipocyte differentiation. The actions of PGE_2 are mediated by four EP subtypes with different signaling pathways [9,10]. However, there has been no literature addressing which EP receptor is involved in the negative regulation of adipocyte differentiation [11]. We recently found that EP4 is the predominant EP receptor expressed in 3T3-L1 preadipocytes, and PGE_2 significantly decreases triglyceride content in cells subjected to a differentiation program, and this inhibition was completely reversed by the addition of an EP4 antagonist [27]. In this study, we used oligonucleotide microarrays to test to what extent PGE_2 inhibits adipocyte

* Corresponding author. Fax: +81 798 41 2792.
E-mail address: aichikaw@mwu.mukogawa-u.ac.jp (A. Ichikawa).
[1] These authors contributed equally to this work.

0006-291X/$ - see front matter © 2004 Elsevier Inc. All rights reserved.
doi:10.1016/j.bbrc.2004.07.194

differentiation and whether EP4 is responsible for its inhibitory action. PGE_2 and an EP4-specific agonist elicited much the same response in 3T3-L1 cells subjected to the differentiation program, and most of these responses were mimicked by treatment with a cAMP analogue. These results suggest that PGE_2 suppresses adipocyte differentiation via EP4 receptor activation and cAMP-dependent signaling.

Materials and methods

Reagents. Dibutyryl cyclic AMP (dbcAMP) was purchased from Sigma (St. Louis, MO). PGE_2 was purchased from Funakoshi (Tokyo, Japan). AE1-329 (an EP4 agonist) was a generous gift from ONO Pharmaceuticals (Osaka, Japan) [12,13]. All other chemicals were commercial products of reagent grade.

Cell culture, RNA isolation, and oligonucleotide microarray. 3T3-L1 preadipocytes were grown to confluence in Dulbecco's modified Eagle's medium (DMEM) supplemented with 10% fetal bovine serum (FBS) and 4 mM glutamine. Differentiation was initiated by addition of the differentiation medium which contained 10% FBS, 4 mM glutamine, 0.5 mM isobutylmethylxanthine (IBMX), 0.25 μM dexamethasone, and 5 μg/ml insulin. After 2 days, the culture medium was changed to adipocyte growth medium containing 10% FBS, 4 mM glutamine, and 5 μg/ml insulin and re-fed every 2 days for an additional 6 days. Vehicle (0.01% ethanol only), PGE_2 (1 μM in 0.01% ethanol), an EP4 agonist, AE1-329 (1 μM in 0.01% ethanol), or dibutyryl cyclic AMP (10 mM in 0.01% ethanol) was added to both the differentiation medium and adipocyte growth medium. Total RNA at each time point was isolated by a combination of the acid guanidinium thiocyanate–phenol–chloroform extraction method [14] and RNeasy column chromatography (Qiagen, Hilden, Germany). The obtained RNA was labeled and prepared for hybridization to GenChip Murine Genome U74v.2 oligonucleotide arrays (Affymetrix, Santa Clara, CA) using standard methods.

Microarray data analysis. We used the robust multi-array analysis (RMA) [15] expression measure that represents the log transform of (background corrected and normalized) intensities of the GeneChips. The RMA measures were computed using the R package program, which is freely available on the web site (http://www.bioconductor.org). We then removed all genes whose maximum minus minimum values were less than 2 (2-fold change), and selected 2268 genes, which were differentially expressed across all samples. Using the *k*-means clustering algorithm, these genes were classified into nine clusters on the basis of similarity of their expression profiles. Since we considered that chronic treatment of the cells with dbcAMP might elicit an excess response in 3T3-L1 cells, the dbcAMP data were used only for consideration of cAMP contribution in the effects of PGE_2 or the EP4 agonist. Microarray analysis was independently repeated at least two times and similar results were obtained.

Results and discussion

We used oligonucleotide microarrays to test to what extent PGE_2 inhibits adipocyte differentiation and whether EP4 is responsible for its inhibitory action. A preadipocyte cell line, 3T3-L1 cells were primed with insulin, dexamethasone, and IBMX for 2 days followed

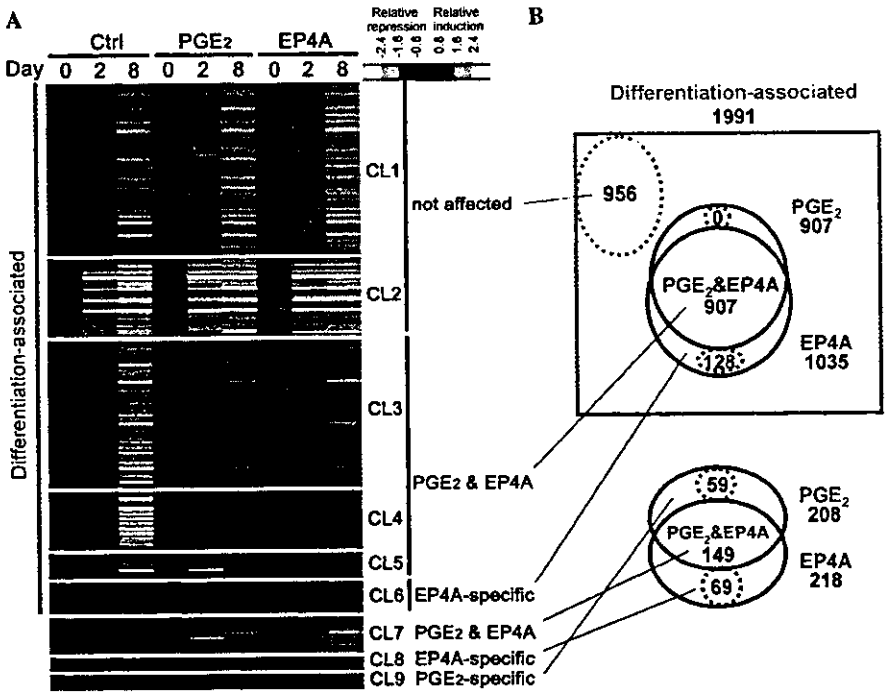

Fig. 1. Differentiation-regulated gene expression in 3T3-L1 preadipocytes. (A) Representation of mRNA expression levels of 3T3-L1 cells on day 2 and 8 of the differentiation program compared with untreated cells (day 0). 3T3-L1 cells grown to confluency were exposed to a differentiation cocktail supplemented with PGE_2 (PGE_2), AE1-329 (EP4A), or vehicle (Ctrl). Each gene is represented by a single row. Colored bars represent the ratio of hybridization measurements between corresponding time points and day 0 profiles, according to the scale shown. (B) Genes are placed in groups corresponding to pairwise overlaps shown in the accompanying Venn diagrams.

by treatment with insulin for an additional 6 days. We isolated total RNA from untreated cells (day 0), the cells on day 2, and day 8 of the differentiation program in the presence or absence of the agonist, and the obtained RNA was labeled and hybridized to microarrays. Of the ~12,000 genes represented on the oligonucleotide array, the genes whose maximum minus minimum values were greater than 2 (2-fold change) were selected, and regarded as differentially expressed genes (2268 genes). Using the *k*-means clustering algorithm, these genes were classified into nine clusters on the basis of similarity of the expression profiles of the day 8 samples treated with PGE_2, AE1-329, and vehicle (control) (Fig. 1). Among them, a total of 1991 genes changed their expression significantly upon standard differentiation treatment (clusters 1–6); 1581 genes were up-regulated (clusters 1, 3, 4, and 6) and 410 genes were down-regulated (clusters 2 and 5). Of such differentiation-associated genes, 956 genes (48%, clusters 1 and 2) were unaffected upon both PGE_2 and AE1-329 treatment (Fig. 1). Since these clusters include a number of genes regulated by insulin such as phosphofructokinase, hexokinase, and glucose transporter 1 (Table 1), an input of EP4 signaling may be ineffective to such a subclass of insulin target genes. On the other hand, differentiation-associated expression changes were inhibited upon treatment with PGE_2 and an EP4 agonist in 907 genes (45.6% of differentiation-associated genes, clusters 3–5), and 231 genes in particular which were drastically induced upon differentiation treatment were completely suppressed by both reagents (cluster 4). It should be noted in cluster 4 that the expression of two key factors which play a central role in adipocyte differentiation, peroxisome proliferator activated receptor-γ (PPARγ), and CCAAT/enhancer binding protein α (C/EBPα), was completely abolished [16,17] (Table 2). PPARγ and C/EBPα were induced by 10.6- and 4.0-fold upon control treatment but PGE_2 inhibited their expression by −7.0- and −4.0-fold, and an EP4 agonist inhibited their expression by −5.3- and −5.0-fold, respectively. Such suppression by both reagents was already observed on day 2 (data not shown). Accordingly, the expression levels of the genes known as differentiation markers were generally lowered upon both agonist treatments; suppression was apparent in the genes encoding adipocytokines (growth hormone releasing hormone, adipsin, resistin, and adiponectin) and enzymes related to lipid metabolism (fatty acid-coenzyme A ligase, diacylglycerol

Table 1
Differentiation-regulated genes insensitive to PGE_2, AE1-329, and dbcAMP

Gene symbol	Gene title	d8ctrl vs d0 $\log_2$(fold)	d8PGE_2 vs d0 $\log_2$(fold)	d8EP4A vs d0 $\log_2$(fold)	d8cAMP vs d0 $\log_2$(fold)	GenBank Accession No.
Cluster 1						
Pfkp	Phosphofructokinase platelet	2.9	2.7	3.0	3.2	AI853802
Hk2	Hexokinase 2	2.8	2.3	2.6	2.6	Y11666
Slc2a1	Solute carrier family 2 (glucose transporter 1)	2.7	2.8	3.0	2.3	M22998
Pla2g12	Phospholipase A2 group XII	2.3	1.7	2.2	1.2	AI845798
Gpi1	Glucose phosphate isomerase 1	2.1	2.2	2.3	2.1	M14220
Pfkl	Phosphofructokinase liver B-type	2.0	1.9	1.9	2.0	J03928
Hmox1	Heme oxygenase 1	2.0	1.6	1.9	1.0	X56824
Facl4	Fatty acid-coenzyme A ligase long chain 4	1.7	2.0	2.3	1.9	AB033887
Adm	Adrenomedullin	1.6	2.2	1.8	1.9	U77630
Pgk1	Phosphoglycerate kinase 1	1.6	1.5	1.7	1.6	M15668
Aldo1	Aldolase 1 A	1.6	1.3	1.4	1.3	AV102160
Cluster 2						
Rpl32	Ribosomal protein L32	−3.7	−3.8	−3.4	−3.4	AV216394
Adam3	A disintegrin and metalloprotease domain 3 (ADAM3)	−3.1	−3.2	−3.5	−3.1	X64227
Coxvib2	Cytochrome *c* oxidase subunit Vib	−3.0	−2.9	−2.9	−2.8	AI893329
Prph1	Peripherin 1	−2.8	−3.0	−2.7	−2.8	X15475
Ogn	Osteoglycin	−2.5	−1.7	−2.1	−2.4	AA647799
Ncam1	Neural cell adhesion molecule 1	−2.3	−2.0	−2.1	−1.8	AV324706
Flnb	Filamin β	−2.2	−2.3	−1.9	−2.1	AV271299
Csf1r	Colony stimulating factor 1 receptor	−2.1	−2.0	−1.6	−1.5	AV028184
Cdh15	Cadherin 15	−2.0	−1.9	−1.9	−1.9	AV232449
Fmod	Fibromodulin	−1.9	−1.8	−1.7	−1.7	AV240231

The list represents differentiation-induced (cluster 1) or differentiation-decreased genes (cluster 2) whose expression levels were unaffected upon PGE_2, AE1-329, and dbcAMP treatment. The change in expression level during the differentiation program for 8 days in the presence of vehicle (d8ctrl), PGE_2 (d8PGE_2), AE1-329 (d8EP4A), and dbcAMP (d8cAMP) is indicated as a logarithm of the fold-change vs the expression level of untreated cells (d0). Representative genes with the largest changes are shown.

Table 2
Differentiation-regulated genes sensitive to PGE_2, AE1-329, and dbcAMP

Gene symbol	Gene title	d8ctrl vs d0 log_2(fold)	d8PGE_2 vs d8ctrl log_2(fold)	d8EP4A vs d8ctrl log_2(fold)	d8cAMP vs d8ctrl log_2(fold)	GenBank Accession No.
Cluster 4						
Fsp27	Fat-specific gene 27	5.6	**−4.4**	**−4.1**	**−4.0**	M61737
Ghrh	Growth hormone releasing hormone	3.2	**−3.4**	**−2.7**	**−2.7**	M31658
Facl2	Fatty acid-coenzyme A ligase long chain 2	4.6	**−2.7**	**−3.3**	**−2.5**	U15977
Adn	Adipsin	5.4	**−3.7**	**−2.2**	**−3.0**	X04673
Pparg	Peroxisome proliferator activated receptor-γ	3.4	**−2.8**	**−2.4**	**−2.4**	U10374
Retn	Resistin	3.0	**−2.6**	**−2.8**	**−2.9**	AA718169
Lipe	Lipase hormone sensitive	3.1	**−2.5**	**−2.5**	**−1.9**	U69543
Acrp30	Adiponectin	5.6	**−2.5**	**−2.2**	**−2.9**	U49915
Cebpa	CCAAT/enhancer binding protein (C/EBP) α	2.0	**−2.0**	**−2.2**	**−1.7**	M62362
Pcx	Pyruvate carboxylase	2.5	**−2.0**	**−2.2**	**−1.6**	M97957
Lpin1	Lipin 1	2.7	**−2.0**	**−1.8**	**−2.3**	AI846934
Ltc4s	Leukotriene C4 synthase	2.7	**−2.0**	**−2.0**	**−1.1**	U27195
Dgat1	Diacylglycerol *O*-acyltransferase 1	3.3	**−1.9**	**−2.0**	**−1.9**	AF078752
Gpd1	Glycerol-3-phosphate dehydrogenase 1	1.8	**−1.9**	**−1.8**	**−1.8**	M25558
Itga6	Integrin α 6	2.8	**−1.8**	**−2.7**	**−2.3**	X69902
Hadhb	Hydroxyacyl-coenzyme A dehydrogenase	2.5	**−1.6**	**−1.8**	**−1.6**	AW122615
Acadm	Acetyl-coenzyme A dehydrogenase medium chain	2.1	**−1.5**	**−1.8**	**−1.9**	U07159
Cat	Catalase	2.5	**−1.5**	**−1.6**	**−1.3**	M29394
Cox7a1	Cytochrome *c* oxidase subunit VIIa 1	1.0	**−1.5**	**−1.4**	**−1.3**	AF037370
Slc25a10	Solute carrier family 25 (dicarboxylate transporter)	1.5	**−1.5**	**−1.3**	**−1.3**	AA683883
Cluster 5						
Gip2	Interferon α-inducible protein	−2.4	**2.0**	**1.6**	**0.8**	AV152244
Ifit3	Interferon-induced protein tetratricopeptide repeats 3	−2.6	**1.5**	**1.2**	**0.9**	U43086
Ifi203	Interferon activated gene 203	−1.2	**1.4**	**0.9**	**0.7**	AF022371
Ifi47	Interferon γ inducible protein	−1.9	**1.4**	**0.9**	**0.5**	M63630
Lox	Lysyl oxidase	−1.0	**1.3**	**1.0**	1.0	D10837
Thbs1	Thrombospondin 1	−1.4	**1.1**	**0.8**	**1.7**	M62470
Ifi202b	Interferon activated gene 202B	−0.9	**1.1**	**0.7**	**0.6**	AV229143
Ifi1	Interferon inducible protein 1	−1.1	**1.1**	**0.6**	**0.4**	U19119
Fbln1	Fibulin 1	−1.3	**1.0**	**0.9**	**1.0**	X70853
Timp2	Tissue inhibitor of metalloproteinase 2	−0.7	**1.0**	**0.6**	**1.0**	X62622

The list represents genes of the differentiation-induced (cluster 4) or differentiation-decreased group (cluster 5) whose changes in expression levels were suppressed upon PGE_2, AE1-329, and dbcAMP treatment (bold values). The change in expression level during control treatment for 8 days (d8ctrl) is indicated as a logarithm of the fold-change vs the expression level of untreated cells (d0), and the effect of PGE_2 (d8PGE_2), AE1-329 (d8EP4A), and dbcAMP (d8cAMP) is indicated as a logarithm of the fold-change vs the expression level of the day 8 control (d8ctrl). Representative genes with the largest changes are shown.

acyltransferase, and hormone sensitive lipase). Moreover, both PGE_2 and an EP4 agonist suppressed responses of the genes negatively regulated upon differentiation treatment (cluster 5); both reagents reversed differentiation-dependent decreases in the expression levels of a number of interferon-γ target genes such as *Ifit3* and *Ifi203*. Since PPARγ has been shown to down-regulate interferon-γ-induced genes in leukocytes [18], an increase in the expression levels of interferon-γ-induced genes was thought to be a result of PGE_2-elicited suppression of PPARγ-dependent signaling. Thus, PGE_2 and an EP4 agonist shared a broad range of suppressive responses especially in differentiation-associated genes, indicating that PGE_2 and an EP4 agonist are equivalent in their inhibitory effect on adipocyte differentiation. Suppression of the differentiation-associated response was also observed in each gene upon treatment with dbcAMP (Table 2). These results indicated that PGE_2 suppresses some crucial step of the adipocyte differentiation process via EP4 receptor activation, presumably in a cAMP-dependent manner. Interestingly, there were a small number of genes that were suppressed by AE1-329 more effectively than by PGE_2 (cluster 6; 128 genes, 6% of the genes with altered expression upon differentiation) (Table 3). It is currently unknown why AE1-329 might affect such genes more effectively than PGE_2, but there may be an induction of EP subtypes subsequently inhibiting EP4 signaling. Indeed, we found that expression of the EP1 receptor gene was induced during the differentiation program [27]. If EP1-induced Ca^{2+} signaling could antagonize EP4-elicited actions, some of the EP4-selective actions could be dismissed in PGE_2 treatment. However, we could not entirely exclude the

Table 3
Differentiation-induced genes preferentially sensitive to an EP4 agonist

Gene symbol	Gene title	d8ctrl vs d0 $\log_2$(fold)	d8PGE_2 vs d8ctrl $\log_2$(fold)	d8EP4A vs d8ctrl $\log_2$(fold)	d8cAMP vs d8ctrl $\log_2$(fold)	GenBank Accession No..
Cluster 6						
Col6a2	Procollagen type VI α 2	0.9	−0.2	**−1.6**	−0.7	Z18272
Kitl	Kit ligand	1.7	−0.1	**−1.6**	−2.3	M57647
Ccnl2	Cyclin L2	1.7	−0.01	**−1.6**	−1.7	U37351
Ier2	Immediate early response 2	0.7	0.04	**−1.1**	−1.1	M59821
Ier5	Immediate early response 5	0.5	0.3	**−1.0**	−0.7	AF079528
Cyp51	Cytochrome P450 51	0.7	−0.2	**−1.0**	−1.1	AW122260
Prkcn	Protein kinase C ν	1.1	0.06	**−0.9**	−0.7	AW124627
Ptges	Prostaglandin E synthase	0.5	0.1	**−0.8**	0.2	AI060798
Ube3a	Ubiquitin protein ligase E3A	0.8	−0.1	**−0.8**	−0.8	U82122
Col4a2	Procollagen type IV α 2	0.9	−0.1	**−0.8**	−0.8	X04647
Col3a1	Procollagen type III α 1	0.5	0.1	**−0.8**	−0.4	AA655199

The list represents differentiation-induced genes whose expression levels were decreased more efficiently by AE1-329 than by PGE_2 (cluster 6, bold values). The change in expression level during the control treatment for 8 days (d8ctrl) is indicated as a logarithm of the fold-change vs the expression level of untreated cells (d0), and the effect of PGE_2 (d8PGE_2), AE1-329 (d8EP4A), and dbcAMP (d8cAMP) is indicated as a logarithm of the fold-change vs the expression level of the day 8 control (d8ctrl). The representative genes with the largest changes are shown.

Table 4
PGE_2- and AE1-329-induced genes not altered upon differentiation treatment

Gene symbol	Gene title	d8ctrl vs d0 $\log_2$(fold)	d8PGE_2 vs d8ctrl $\log_2$(fold)	d8EP4A vs d8ctrl $\log_2$(fold)	d8cAMP vs d8ctrl $\log_2$(fold)	GenBank Accession No.
Cluster 7						
Cmkorl	Chemokine orphan receptor 1	0.2	**1.8**	**1.5**	3.3	AF000236
Aqp1	Aquaporin 1	−0.2	**1.3**	**1.3**	1.0	L02914
Gja1	Gap junction membrane channel protein α 1	0.3	**1.2**	**1.7**	3.0	M63801
Ptgs1	Prostaglandin-endoperoxide synthase 1 (COX-1)	−0.04	**1.1**	**0.8**	1.1	M34141
Gla	Galactosidase α	−0.3	**1.0**	**1.6**	1.4	L46651
Procr	Protein C receptor endothelial	−0.3	**1.0**	**1.5**	0.9	L39017
Psmb8	Proteosome subunit β type 8	−0.09	**0.8**	**1.2**	0.8	U22033
Fkbp11	FK506 binding protein 11	−0.3	**0.8**	**1.1**	0.6	AW122851
Ptgs2	Prostaglandin-endoperoxide synthase 2 (COX-2)	0.2	**0.8**	**1.0**	1.4	M88242
Pla2g7	Phospholipase A2 VII (PAF acetylhydrolase)	−0.1	**0.8**	**0.8**	0.5	U34277
Timp1	Tissue inhibitor of metalloproteinase 1	−0.3	**0.7**	**0.5**	1.7	V00755
Pla2g4a	Phospholipase A2 group IVA (cPLA2)	−0.1	**0.6**	**0.6**	0.3	M72394

The list represents differentiation-independent genes whose expression levels were increased both by AE1-329 and PGE_2 (cluster 7, bold values). The change in expression level during control treatment for 8 days (d8ctrl) is indicated as a logarithm of the fold-change vs the expression level of untreated cells (d0), and the effect of PGE_2 (d8PGE_2), AE1-329 (d8EP4A), and dbcAMP (d8cAMP) is indicated as a logarithm of the fold-change vs the expression level of the day 8 control (d8ctrl). Representative genes with the largest changes are shown.

possibility that the non-agonistic nature of AE1-329 may alter the expression levels of the genes in cluster 6.

On the other hand, either agonist treatment also affected expression levels in a group of genes not altered upon differentiation treatment. For example, both PGE_2 and AE1-329 increased the expression levels of a class of genes (cluster 7; 149 genes) (Table 4). This group includes rate-limiting enzymes of PG synthesis; prostaglandin-endoperoxide synthase 1 (COX-1), COX-2, and cytosolic phospholipase A_2. Since such genes were also up-regulated upon dbcAMP treatment, PGE_2 may stimulate endogenous PG synthesis by EP4 receptor activation and the resultant increase in intracellular cAMP. Such positive-feedback regulation in PGE_2 actions, which has been described in other systems [19,20], may contribute to the inhibitory actions of PGE_2 on differentiation. Moreover, a group of genes were down-regulated by AE1-329 more efficiently than by PGE_2 (cluster 8; 59 genes) (Table 5). In contrast, a small group of genes was up-regulated by PGE_2 more efficiently than AE1-329 (cluster 9; 69 genes). The existence of genes showing different responses to an EP4 agonist and to PGE_2 may be due to a non-agonistic or toxic effect of AE1-329, because the effect of the agonist was not always mimicked by dbcAMP in these genes.

PGs have long been thought to contribute to fat cell development, but the role of PGs in the regulation of adipocyte differentiation is complex and remains unclear [11]. One of the reasons of its complexity is that different classes of PGs exert opposing effects on differentiation.

Table 5
PGE_2-induced or AE1-329-decreased genes not associated with differentiation

Gene symbol	Gene title	d8ctrl vs d0 log_2(fold)	d8PGE_2 vs d8ctrl log_2(fold)	d8EP4A vs d8ctrl log_2(fold)	d8cAMP vs d8ctrl log_2(fold)	GenBank Accession No.
Cluster 8						
Cyp1b1	Cytochrome P450 family 1 subfamily b 1	0.2	−0.1	**−1.3**	−0.7	X78445
Pftk1	PFTAIRE protein kinase 1	0.2	0.1	**−1.1**	−0.7	AF033655
Fgfr2	Fibroblast growth factor receptor 2	0.2	−0.1	**−0.9**	−0.7	M23362
Rin2	Ras and Rab interactor 2	0.1	0.1	**−0.9**	−0.1	AI835968
Il1r1	Interleukin 1 receptor type I	0.2	0.3	**−0.9**	−0.2	M20658
Agpt	Angiopoietin	0.1	0.4	**−0.9**	−0.2	U83509
Nfib	Nuclear factor I/B	0.2	0.2	**−0.7**	−1.2	Y07686
Cxcl12	Chemokine (C-X-C motif) ligand 12	−0.2	0.4	**−0.6**	−0.7	L12029
Skd3	Suppressor of K^+ transport defect 3	0.1	0.4	**−0.6**	−0.2	AI837887
Cluster 9						
Timp3	Tissue inhibitor of metalloproteinase 3	0.2	**1.6**	0.3	1.1	U26437
Rbp1	Retinol binding protein 1 cellular	−0.2	**1.4**	0.4	2.3	X60367
Cdh2	Cadherin 2	−0.1	**0.9**	0	0.5	M31131
Col1a1	Procollagen type I α 1	0.1	**0.8**	−0.1	0.2	U03419
Hgf	Hepatocyte growth factor	0.2	**0.7**	0.1	1.6	X72307
Vdr	Vitamin D receptor	−0.1	**0.6**	0.1	1.6	AW061016
Pip	Prolactin induced protein	−0.1	**0.6**	0.1	1.3	AB017918
Angptl2	Angiopoietin-like 2	0	**0.5**	0	1.2	AI840158
Ereg	Epiregulin	0.2	**0.5**	0	0.8	D30782

The list represents differentiation-independent genes whose expression levels were decreased only by AE1-329 (cluster 8, bold values) or induced only by PGE_2 (cluster 9, bold values). The change in expression level during control treatment for 8 days (d8ctrl) is indicated as a logarithm of the fold-change vs the expression level of untreated cells (d0), and the effect of PGE_2 (d8PGE_2), AE1-329 (d8EP4A), and dbcAMP (d8cAMP) is indicated as a logarithm of the fold-change vs the expression level of the day 8 control (d8ctrl). Representative genes with the largest changes are shown.

For example, both PGI_2 and PGE_2, the two PGs predominantly synthesized by fat cells, appear to have opposing effects on early adipogenesis [21,22]; PGI_2 promotes adipocyte differentiation, whereas PGE_2 inhibits differentiation. We hypothesized that the complex role of PGs in adipogenesis may be explained by the expression of multiple prostanoid receptors in preadipocytes. Indeed, we [27] as well as another group have found the expression of multiple PG receptor genes in 3T3-L1 cells [23]. The current results indicate that PGE_2 and an EP4-specific agonist share much the same response in 3T3-L1 cells with differentiation-reversed profiles, suggesting that PGE_2 suppresses adipocyte differentiation via EP4 receptor activation and cAMP-dependent signaling. Indeed, requirement of a cAMP-dependent pathway in arachidonic acid-dependent inhibition of adipocyte differentiation has been pointed out [24]. Recently, Yokota et al. [25] demonstrated that adiponectin, one of the adipocytokines secreted from fat cells, exerts an inhibitory effect on adipocyte differentiation as a negative-feedback loop. Interestingly, they suggested that this effect of adiponectin is mediated by an endogenous COX-2- and PGE_2-dependent pathway. Moreover, Yan et al. [26] reported that both a COX-1- and COX-2-inhibitor enhances differentiation of 3T3-L1 cells, indicating that both COX isozymes participate in the negative regulation of adipogenesis. Involvement of EP4 signaling in these systems is an interesting issue to be examined in the future.

Acknowledgments

This work was supported in part by a grant from the Sankyo Foundation of Life Science, and Grants-in-Aid for Scientific Research on Priority Areas from the Ministry of Education, Culture, Sports, Science and Technology of Japan and from the Ministry of Health and Labor of Japan. We thank Drs. S. Narumiya and E. Segi for their kind instruction on the Affymetrix GenChip system, and also thank Drs. M. Imagawa and S. Tanaka for their invaluable advice on this study. We are grateful to Dr. Helena A. Popiel, and Ms. Sachiko Terai-Yamaguchi for careful reading and secretary assistance.

References

[1] F.M. Gregoire, C.M. Smas, H.S. Sul, Understanding adipocyte differentiation, Physiol. Rev. 78 (1998) 783–809.
[2] E.D. Rosen, B.M. Spiegelman, Molecular regulation of adipogenesis, Annu. Rev. Cell Dev. Biol. 16 (2001) 145–171.
[3] P.B. Curtis-Prior, Prostaglandins and obesity, Lancet 1 (1975) 897–899.
[4] I.H. Williams, S.E. Polakis, Differentiation of 3T3-L1 fibroblasts to adipocytes. The effect of indomethacin, prostaglandin E1 and cyclic AMP on the process of differentiation, Biochem. Biophys. Res. Commun. 77 (1977) 175–186.
[5] P. Verrando, R. Negrel, P. Grimaldi, M. Murphy, G. Ailhaud, Differentiation of ob 17 preadipocytes to adipocytes. Triggering

effects of clofenapate and indomethacin, Biochim. Biophys. Acta 663 (1981) 255–265.
[6] D.A. Casimir, C.W. Miller, J.M. Ntambi, Preadipocyte differentiation blocked by prostaglandin stimulation of prostanoid FP2 receptor in murine 3T3-L1 cells, Differentiation 60 (1996) 203–210.
[7] C.W. Miller, D.A. Casimir, J.M. Ntambi, The mechanism of inhibition of 3T3-L1 preadipocyte differentiation by prostaglandin F2alpha, Endocrinology 137 (1996) 5641–5650.
[8] J.N. Fain, L.R. Ballou, S.W. Bahouth, Obesity is induced in mice heterozygous for cyclooxygenase-2, Prostaglandins Other Lipid Mediat. 65 (2001) 199–209.
[9] M. Negishi, Y. Sugimoto, A. Ichikawa, Prostaglandin E receptors, J. Lipid Mediat. Cell Signal. 12 (1995) 379–391.
[10] Y. Sugimoto, S. Narumiya, A. Ichikawa, Distribution and function of prostanoid receptors: studies from knockout mice, Prog. Lipid Res. 39 (2000) 289–314.
[11] S. Kim, N. Moustaid-Moussa, Secretory, endocrine and autocrine/paracrine function of the adipocyte, J. Nutr. 130 (2000) 3110S–3115S.
[12] T. Suzawa, C. Miyaura, M. Inada, T. Maruyama, Y. Sugimoto, F. Ushikubi, A. Ichikawa, S. Narumiya, T. Suda, The role of prostaglandin E receptor subtypes (EP1, EP2, EP3 and EP4) in bone resorption: an analysis using specific agonists for the respective EPs, Endocrinology 141 (2000) 1554–1559.
[13] K. Yoshida, H. Oida, T. Kobayashi, T. Maruyama, M. Tanaka, T. Katayama, K. Yamaguchi, E. Segi, T. Tsuboyama, M. Matsushita, K. Ito, Y. Ito, Y. Sugimoto, F. Ushikubi, S. Ohuchida, K. Kondo, T. Nakamura, S. Narumiya, Stimulation of bone formation and prevention of bone loss by prostaglandin E EP4 receptor activation, Proc. Natl. Acad. Sci. USA 99 (2002) 4580–4585.
[14] P. Chomczynski, N. Sacchi, Single-step method of RNA isolation by acid guanidinium thiocyanate-phenol-chloroform extraction, Anal. Biochem. 162 (1987) 156–159.
[15] R.A. Irizarry, B.M. Bolstad, F. Collin, L.M. Cope, B. Hobbs, T.P. Speed, Summaries of Affymetrix GeneChip probe level data, Nucleic Acids Res. 31 (2003) e15.
[16] P. Tontonoz, E. Hu, B.M. Spiegelman, Regulation of adipocyte gene expression and differentiation by peroxisome proliferator activated receptor gamma, Curr. Opin. Genet. Dev. 5 (1995) 571–576.
[17] H.S. Camp, D. Ren, T. Leff, Adipogenesis and fat-cell function in obesity and diabetes, Trends Mol. Med. 8 (2002) 442–447.
[18] J.S. Welch, M. Ricote, T.E. Akiyama, F.J. Gonzalez, C.K. Glass, PPARgamma and PPARdelta negatively regulate specific subsets of lipopolysaccharide and IFN-gamma target genes in macrophages, Proc. Natl. Acad. Sci. USA 100 (2003) 6712–6717.
[19] T. Oshima, T. Yoshimoto, S. Yamamoto, M. Kumegawa, C. Yokoyama, T. Tanabe, cAMP-dependent induction of fatty acid cyclooxygenase mRNA in mouse osteoblastic cells (MC3T3-E1), J. Biol. Chem. 266 (1991) 13621–13626.
[20] Y. Takahashi, Y. Taketani, T. Endo, S. Yamamoto, M. Kumegawa, Studies on the induction of cyclooxygenase isozymes by various prostaglandins in mouse osteoblastic cell line with reference to signal transduction pathways, Biochim. Biophys. Acta 1212 (1994) 217–224.
[21] G. Vassaux, D. Gaillard, G. Ailhaud, R. Negrel, Prostacyclin is a specific effector of adipose cell differentiation. Its dual role as a cAMP- and Ca(2+)-elevating agent, J. Biol. Chem. 267 (1992) 11087–11092.
[22] G. Vassaux, D. Gaillard, C. Darimont, G. Ailhaud, R. Negrel, Differential response of preadipocytes and adipocytes to prostacyclin and prostaglandin E2: physiological implications, Endocrinology 131 (1992) 2393–2398.
[23] J.D. Borglum, S.B. Pedersen, G. Ailhaud, R. Negrel, B. Richelsen, Differential expression of prostaglandin receptor mRNAs during adipose cell differentiation, Prostaglandins Other Lipid Mediat. 57 (1999) 305–317.
[24] R.K. Petersen, C. Jorgensen, A.C. Rustan, L. Froyland, K. Muller-Decker, G. Furstenberger, R.K. Berge, K. Kristiansen, L. Madsen, Arachidonic acid-dependent inhibition of adipocyte differentiation requires PKA activity and is associated with sustained expression of cyclooxygenases, J. Lipid Res. 44 (2003) 2320–2330.
[25] T. Yokota, C.S. Meka, K.L. Medina, H. Igarashi, P.C. Comp, M. Takahashi, M. Nishida, K. Oritani, J. Miyagawa, T. Funahashi, Y. Tomiyama, Y. Matsuzawa, P.W. Kincade, Paracrine regulation of fat cell formation in bone marrow cultures via adiponectin and prostaglandins, J. Clin. Invest. 109 (2002) 1303–1310.
[26] H. Yan, A. Kermouni, M. Abdel-Hafez, D.C. Lau, Role of cyclooxygenases COX-1 and COX-2 in modulating adipogenesis in 3T3-L1 cells, J. Lipid Res. 44 (2003) 424–429.
[27] H. Tsuboi, Y. Sugimoto, T. Kainoh, A. Ichikawa. Prostanoid EP4 receptor is involved in suppression of 3T3-L1 adipocyte differentiation. Biochem. Biophys. Res. Commun. 322 (2004), in press.

THE JOURNAL OF BIOLOGICAL CHEMISTRY
Vol. 279, No. 12, Issue of March 19, pp. 11016–11026, 2004
Printed in U.S.A.

A Cluster of Aromatic Amino Acids in the i2 Loop Plays a Key Role for G_s Coupling in Prostaglandin EP2 and EP3 Receptors*

Received for publication, July 10, 2003, and in revised form, December 28, 2003
Published, JBC Papers in Press, December 29, 2003, DOI 10.1074/jbc.M307404200

Yukihiko Sugimoto‡, Toshiyuki Nakato‡, Ayumi Kita‡, Yuko Takahashi, Noriyuki Hatae, Hiroyuki Tabata, Satoshi Tanaka, and Atsushi Ichikawa§

From the Department of Physiological Chemistry, Graduate School of Pharmaceutical Sciences, Kyoto University, Sakyo-ku, Kyoto 606-8501, Japan

To assess the structural requirements for G_s coupling by prostaglandin E receptors (EPs), the G_s-coupled EP2 and G_i-coupled EP3β receptors were used to generate hybrid receptors. Interchanging of the whole i2 loop and its N-terminal half (i2N) had no effect on the binding of both receptors expressed in HEK293 cells. Agonist-induced cAMP formation was observed in wild type EP2 but not in the i2 loop- or i2N-substituted EP2. Wild type EP3β left cAMP levels unaffected, whereas i2 loop- and i2N-substituted EP3 gained agonist-induced adenylyl cyclase stimulation. In EP2, the ability to stimulate cAMP formation was lost by mutation of Tyr^{143} into Ala but retained by mutations into Phe, Trp, and Leu. Consistent with this observation, substitution of the equivalent His^{140} enabled EP3β to stimulate cAMP formation with the rank order of Phe > Tyr > Trp > Leu. The point mutation of His^{140} into Phe was effective in another EP3 variant in which its C-terminal tail is different or lacking. Simultaneous mutation of the adjacent Trp^{141} to Ala but not at the following Tyr^{142} weakened the acquired ability to stimulate cAMP levels in the EP3 mutant. Mutation of EP2 at adjacent Phe^{144} to Ala but not at Tyr^{145} reduced the efficiency of agonist-induced cAMP formation. In Chinese hamster ovary cells stably expressing G_s-acquired EP3 mutant, an agonist-dependent cAMP formation was observed, and pertussis toxin markedly augmented cAMP formation. These results suggest that a cluster of hydrophobic aromatic amino acids in the i2 loop plays a key role for G_s coupling.

Individual members of the superfamily of G protein-coupled receptors (GPCRs)[1] efficiently interact only with a subset of the many structurally similar G protein heterotrimers (1–3). The spectrum of cellular responses triggered by activation of a specific GPCR is determined by the type of G proteins recognized by the activated receptor. It is therefore very important to elucidate the molecular basis governing the selectivity of receptor/G protein interaction for understanding cellular signal transduction.

Accumulating evidence indicates that multiple receptor regions of GPCRs are involved in G protein coupling and determining the selectivity of G protein recognition. Numerous studies have shown that the second intracellular loop (i2 loop), the membrane-proximal portions of the third intracellular loop (i3 loop), and the N-terminal segment of the cytoplasmic tail all contain amino acids predicted to play roles in regulating selectivity of receptor/G protein interactions (4, 5). Traditional mutagenesis approaches, including the use of hybrid receptors and alanine-scanning mutagenesis techniques, have led to important insights into the structural basis underlying the selectivity of receptor/G protein interactions (6). For example, intracellular loop 1 (i1 loop) is less important in determination of G protein selectivity but may indirectly contribute to G protein recognition. The i2 loop and i3 loop are of critical importance in determining the selectivity of receptor/G protein coupling and the efficiency of G-protein activation. The C-terminal tail plays a role in constraining basal activity, by preventing access of the G-protein to the receptor surface. Despite such information, it still remains controversial which receptor elements are critical for G protein selectivity and activation, and thus it is still difficult to predict whether a particular receptor can couple to a G protein.

Prostaglandin E_2 (PGE_2), one of the best known arachidonate metabolites, exhibits a broad range of biological actions in diverse tissues through their binding to specific receptors on the plasma membrane (7). We and other groups have revealed the primary structures of eight types of prostanoid receptors, including four subtypes of PGE receptors (EP1, EP2, EP3, and EP4), and demonstrated that they belong to the subfamily of rhodopsin-type (class I) GPCRs (8, 9). Prostanoid receptors thus have several unique features specific to prostanoid receptors in addition to those in common with other rhodopsin-type receptors; for example, they contain fewer basic or acidic amino acids throughout their putative transmembrane domains (10). To assess the roles of such unique structural features, we have investigated the properties of receptors with mutations within such unique regions and demonstrated that the arginine residue within the putative seventh transmembrane domain conserved in all prostanoid receptors is important not only for interaction with the carboxylic acid group of agonists but also for particular signal activation (11–14). Furthermore, we found that the aspartate residue within the seventh transmembrane domain of the EP3 receptor plays a key role in governing G protein association and activation (15). On the other hand,

* This work was supported in part by grants from the Sankyo Foundation of Life Science and the Takeda Science Foundation, Health and Labor Sciences research grants, and Grants-in-aid for Scientific Research 12139205, 15012234, 15019050, and 15390024 from the Ministry of Education, Culture, Sports Science and Technology of Japan. The costs of publication of this article were defrayed in part by the payment of page charges. This article must therefore be hereby marked "*advertisement*" in accordance with 18 U.S.C. Section 1734 solely to indicate this fact.

‡ These authors contributed equally to this work.

§ To whom correspondence should be addressed: School of Pharmaceutical Sciences, Mukogawa Women's University, 11-68, Kyuban-chou, Koshien, Nishinomiya, Hyogo 663-8179, Japan. Tel.: 81-798-45-9947; Fax: 81-798-41-2792; E-mail: aichikaw@mwu.mukogawa-u.ac.jp.

[1] The abbreviations used are: GPCR, G protein-coupled receptor; PGE_2, prostaglandin E_2; PT, pertussis toxin; i1–i3, the three intracellular domains of G protein-coupled receptors; TM I–VII, first to seventh transmembrane domains; Mes, 4-morpholineethanesulfonic acid; CHO, Chinese hamster ovary.

multiple EP3 receptor isoforms exist, which are different only in their C-terminal structures (16, 17). We found that these isoforms are different in their constitutive G_i activities and thus concluded that the C-terminal tail plays a role in constraining the basal activity, by preventing access of the G_i to the receptor surface (18–21). Thus, structurally close members of the GPCR subfamily such as the prostanoid receptors are useful not only for understanding prostanoid receptor-specific events but also for elucidating the general molecular basis of the structure and function relationship of GPCRs, including G protein selectivity.

To gain new insight into the mechanisms governing receptor/G protein coupling selectivity, here we designed a series of experiments using two members of the prostanoid receptors, aiming to identify structural requirements for selective G_s coupling. We first constructed G_s-coupled EP2 and G_i-coupled EP3 hybrid receptors with the i1, i2, or i3 loops interchanged and examined possible functional interchanges in G_s coupling in these mutant receptors. Second, we searched for the functional amino acids critical for G_s coupling.

EXPERIMENTAL PROCEDURES

Materials—Sulprostone and butaprost were generous gifts from Dr. M. P. L. Caton of Rhone-Poulenc Ltd. [5,6,8,11,12,14,15-^{3}H]PGE_2 (185 Ci/mmol) and a ^{125}I-labeled cAMP assay system were obtained from Amersham Biosciences. Forskolin was from Sigma, and pertussis toxin was from Seikagaku (Tokyo, Japan). All other chemicals were of reagent grade.

Construction of cDNAs for the mEP2, mEP3β, EP2-based, and EP3-based Mutant Receptors—The functional cDNAs for mouse EP2 (mEP2), EP3β (mEP3β), EP3γ, and T335 were previously cloned or generated in our laboratory (16, 22). The construction of pcDNA3-based expression plasmids (Invitrogen) encoding for wild-type mEP2 and mEP3β has been described previously (23). Various EP2/EP3 chimeric receptors and various mutant EP2 and EP3 receptors were prepared by standard PCR-based mutagenesis techniques (QuikChange™ site-directed mutagenesis kit; Stratagene, La Jolla, CA). For EP2-based chimeras, the following mEP2 receptor sequences were replaced with the corresponding mEP3β receptor segments: EP2-i1, mEP2 47–67 → mEP3β 50–64; EP2-i2, mEP2 136–151 → mEP3β 133–148; EP2-i3, mEP2 222–262 → mEP3β 231–256; EP2-i2N, mEP2 136–143 → mEP3β 133–140; EP2-i2C, mEP2 144–151 → mEP3β 141–148. For EP3-based chimeras, the following mEP3β receptor sequences were replaced with the corresponding mEP2 receptor segments; EP3-i1, mEP3β 50–64 α mEP2 47–67; EP3-i2, mEP3β 133–148 → mEP2 136–151; EP3-i3, mEP3β 231–256 → mEP2 222–262; EP3-i2N, mEP3β 133–140 → mEP2 136–143; EP3-i2C, mEP3β 141–148 → mEP2 144–151. Single amino acid substitutions in mEP2, mEP3β, EP3γ, and T335 were introduced in a similar manner. All PCR-derived sequences were verified by dideoxy sequencing of the mutant plasmids.

Cell Culture, Transient Expression, and Surface Expression of EP2-based or EP3-based Mutant Receptors in HEK293 Cells—HEK293 cells were maintained in Dulbecco's modified Eagle's medium with 10% heat-inactivated fetal bovine serum under humidified air containing 5% CO_2 at 37 °C. For transfection using the LipofectAMINE 2000 reagent (Invitrogen), cells in 60-mm tissue culture dishes were incubated at 37 °C for 4 h with a transfection mixture composed of 3 ml of Dulbecco's modified Eagle's medium, containing 10% heat-inactivated fetal bovine serum, 1 μg of DNA, and 15 μl of LipofectAMINE 2000 reagent. For the cAMP assay, HEK293 cells were then trypsinized, and aliquots of recovered cells were transferred to 24-well tissue culture plates. Surface expression of receptor proteins on HEK cell membranes was confirmed by an immunofluorescence assay using antibodies against the N-terminal region of the mouse EP2 and EP3 receptors under nonpermeabilized conditions.

PGE_2-binding Assay—The harvested HEK293 cells expressing each receptor were homogenized using a Potter-Elvehjem homogenizer in 20 mM Tris-HCl (pH 7.5), containing 10 mM $MgCl_2$, 1 mM EDTA, 20 μM indomethacin, and 0.1 mM phenylmethylsulfonyl fluoride. After centrifugation at 250,000 × *g* for 20 min, the pellet was washed, suspended in 20 mM Mes-NaOH (pH 6.0) containing 10 mM $MgCl_2$ and 1 mM EDTA, and was used for the [^{3}H]PGE_2-binding assay. The membranes (50 μg) were incubated with various concentrations of [^{3}H]PGE_2 at 30 °C for 1 h, and [^{3}H]PGE_2 binding to the membranes was determined by adding a 1000-fold excess of unlabeled PGE_2 into the incubation mixture. The specific binding was calculated by subtracting the nonspecific binding from the total binding.

Measurement of cAMP Formation—Cyclic AMP levels in HEK293 cells were determined as reported previously (24). The receptor-expressing HEK293 cells cultured in 24-well plates (2×10^5 cells/well) were washed with HEPES-buffered saline containing 140 mM NaCl, 4.7 mM KCl, 2.2 mM $CaCl_2$, 1.2 mM $MgCl_2$, 1.2 mM KH_2PO_4, 11 mM glucose, 10 μM indomethacine, and 15 mM HEPES, pH 7.4, and preincubated for 10 min. Reactions were started by the addition of test reagents along with 100 μM Ro-20–1724. After incubation for 10 min at 37 °C, reactions were terminated by the addition of 10% trichloroacetic acid. The content of cAMP in the cells was measured by radioimmunoassay with a cAMP assay system (Amersham Biosciences).

Stable Expression of mEP3β, EP3-H140F, mEP2, and EP2-Y143A in the Chinese Hamster Ovary (CHO) Cells—cDNAs for mEP3β, EP3-H140F, mEP2, and EP2-Y143A were transfected into CHO cells using the LipofectAMINE PLUS system according to the manufacturer's instructions, and stable transformants were cloned as described previously (16). CHO cells expressing each receptor (5×10^5 cells) were pretreated with or without PT (20 ng/ml) for 7 h before the addition of the agonist. The cells expressing EP3 receptors were incubated at 37 °C for 10 min with or without sulprostone in the absence or presence of 10 μM forskolin. The cells expressing EP2 receptors were incubated at 37 °C for 10 min with or without butaprost. The cAMP contents were determined as described above.

Statistical Analysis—All data shown are expressed as means ± S.E. of three independent experiments. Statistical analysis was carried out by Student's *t* test. *p* values of <0.005 were considered to indicate a significant difference.

RESULTS

Agonist Binding Properties in Hybrid EP2-EP3 Receptors—Wild type and mutant EP receptors analyzed in this study were transiently expressed in HEK293 cells and assayed for their ability to mediate agonist-dependent stimulation of adenylyl cyclase (mediated by G_s). Consistent with its reported profile, the wild-type EP2 receptor (mouse, mEP2) caused a pronounced increase in intracellular cAMP levels upon stimulation with butaprost, an EP2 agonist. On the other hand, sulprostone stimulation of the wild type EP3β receptor (mouse, mEP3β) left cAMP levels unaffected. To explore the structural basis underlying G_s coupling, a series of hybrid EP2/EP3 receptors were created in which the intracellular domains were systematically exchanged between the two wild type receptors (Fig. 1*A*). EP2-i1 and EP3-i1 represent EP2 and EP3β with interchanged i1 loops, respectively. Moreover, we created hybrid receptors in which the N-terminal (i2N) or C-terminal halves of the i2 loops (i2C) were individually exchanged between the wild type receptors as described below. For every mutant receptor used in this study, the expression of receptor proteins in HEK293 cells was examined by immunofluorescent analysis using antibodies against the N-terminal region of the mouse EP2 and EP3 receptors under nonpermeabilized conditions, and membrane surface expression and the expression levels of each mutant receptor were found to be comparable with those of wild-type receptors (Fig. 1*A* and data not shown).

Saturation binding studies showed that among the EP2-based hybrid receptors, EP2-i2, EP2-i2N, and EP2-i2C retained the ability to bind to the agonist [^{3}H]PGE_2 with high affinity, but EP2-i1 and EP2-i3 failed to bind to the agonist (Table I). The EP2-i2, EP2-i2N, and EP2-i2C hybrid receptors exhibited K_d values close to that obtained for the wild type EP2 receptor (Table I). [^{3}H]PGE_2 binding to these mutants was displaced by the addition of butaprost with K_i values similar to that of the wild type EP2 receptor (K_i for butaprost, 1.7–3.0 μM). These three hybrid receptors were expressed at levels similar to that found for the wild-type EP2 receptor (B_{max} = 803–1110 fmol/mg; Table I). On the other hand, all EP3-based hybrid receptors except for EP3-i1 retained the ability to bind to [^{3}H]PGE_2. These hybrid receptors exhibited K_d values close to that ob-

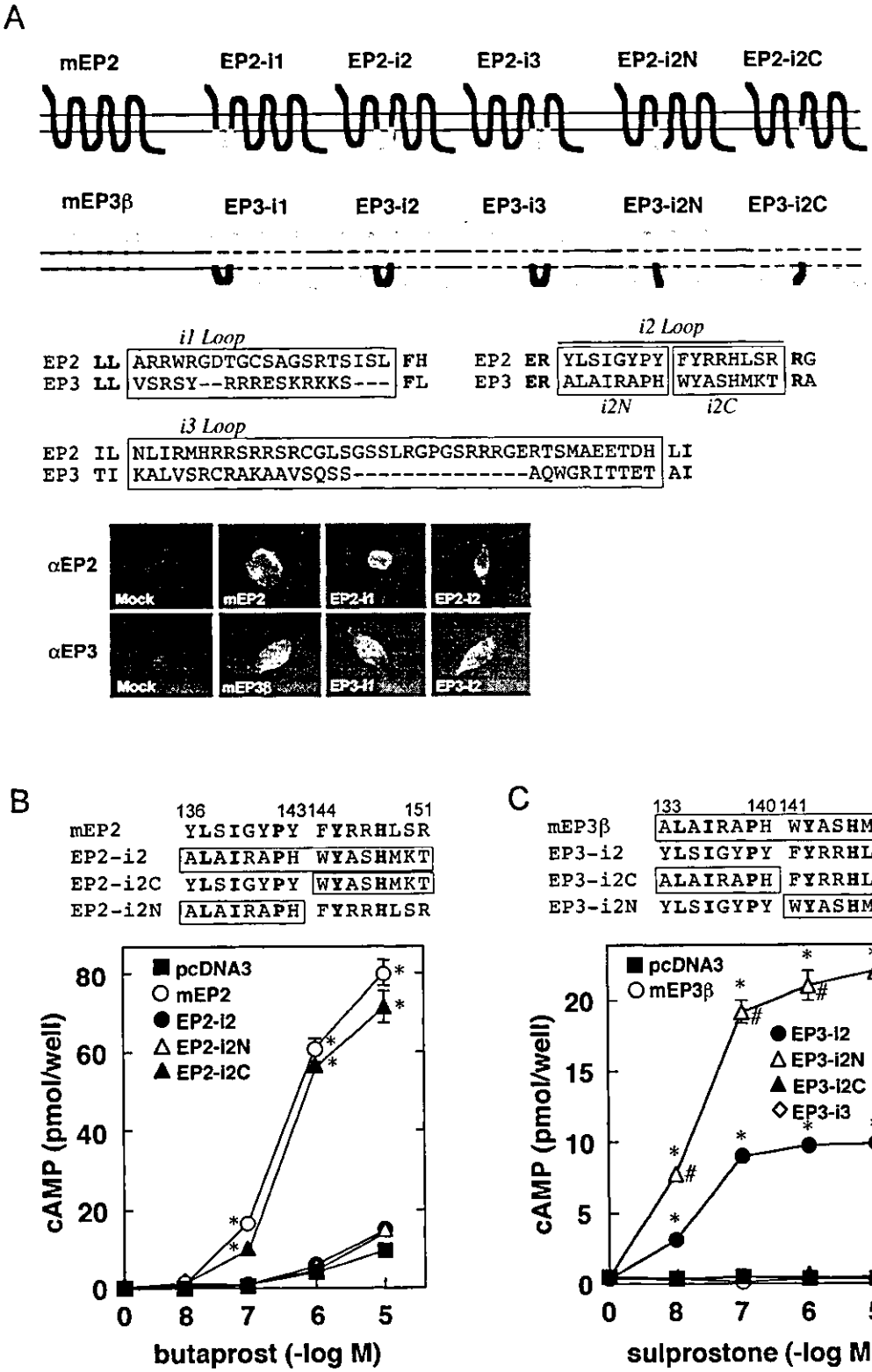

FIG. 1. **Structures and agonist-dependent G_s activities of EP2/EP3 hybrid receptors.** *A*, diagrams showing structures of mEP2, mEP3β, and the 10 mutant receptors used in this study and immunocytochemistry showing surface expression of the wild-type receptors and their chimeras. The part of the receptors derived from mEP2 is shown in *black*, and that from mEP3β is shown in *gray*. The amino acid sequences of the i1–i3 loops of EP2 and EP3 are shown *below* the *diagrams*, and the region interchanged between the two receptors is *boxed*. Extracellular N-terminal sequences were detected using corresponding antibodies on nonpermeabilized transfected HEK293 cells. The surface expression was visualized using secondary antibodies labeled by fluorescence. Background was compared using cells transfected with empty vector, pcDNA3 (*Mock*). *B* and *C*, agonist-dependent cAMP formation in HEK293 cells expressing mEP2 and EP2-based mutant receptors (*B*) and in HEK 293 cells expressing mEP3β and EP3-based mutant receptors (*C*). HEK293 cells expressing each receptor or pcDNA3-transfected HEK293 cells were seeded and cultured for 24 h before the assay (2×10^5 cells/well). For the mEP2 and EP2-based mutant receptors, the cells were stimulated for 10 min by adding media with the indicated concentrations of butaprost, an EP2-selective agonist (*B*). For the mEP3β and EP3-based mutant receptors, the cells were stimulated for 10 min by adding media with the indicated concentrations of sulprostone, an EP3-selective agonist (*C*). Amino acid

TABLE I

Summary of binding properties in mEP2, mEP3β, and their mutant receptors

The binding activities for [^{3}H]PGE_2 of mEP2, mEP3β and the mutant receptors expressed in HEK293 cells were assessed by Scatchard plot analysis, and the K_d and B_{max} values are shown. NP, not performed; ND, not detected (for the EP2-based and EP3-based mutant receptors).

Receptor	K_d	B_{max}	K_i for selective agonist[a]
	nM	*fmol/mg protein*	*μM or nM*
mEP2	19.2 ± 2.1	934 ± 97	1.8 ± 0.09
EP2-i1	ND	ND	NP
EP2-i2	23.3 ± 1.1	1110 ± 83	2.2 ± 0.11
EP2-i3	ND	ND	NP
EP2-i2N	16.2 ± 1.4	1040 ± 96	1.7 ± 0.15
EP2-i2C	12.2 ± 1.8	803 ± 71	3.0 ± 0.12
EP2-Y143A	32.0 ± 2.9	709 ± 82	3.3 ± 0.29
EP2-Y143F	19.4 ± 2.2	638 ± 65	2.3 ± 0.18
EP2-Y143W	21.1 ± 1.7	749 ± 38	2.0 ± 0.51
EP2-YAA	12.8 ± 2.0	110 ± 14	NP
mEP3β	2.24 ± 0.33	1680 ± 123	4.3 ± 0.18
EP3-i1	ND	ND	NP
EP3-i2	1.53 ± 0.21	1520 ± 142	1.5 ± 0.09
EP3-i3	1.43 ± 0.18	1503 ± 64	1.1 ± 0.10
EP3-i2N	2.89 ± 0.32	1610 ± 105	2.3 ± 0.15
EP3-i2C	1.99 ± 0.13	1920 ± 99	3.1 ± 0.24
EP3-H140Y	3.14 ± 0.26	1010 ± 118	4.0 ± 0.39
EP3-H140F	2.68 ± 0.26	1092 ± 95	3.6 ± 0.78
EP3-H140A	3.23 ± 0.35	1170 ± 87	2.9 ± 0.49
EP3-YAA	1.86 ± 0.22	1840 ± 124	NP

[a] K_i values for butaprost (μM) and for sulprostone (nM) are indicated, respectively.

tained for the wild type EP3 receptor (Table I). [^{3}H]PGE_2 binding to EP3-i2, EP3-i3, EP3-i2N, and EP3-i2C was displaced by the addition of sulprostone with K_i values similar to that of the wild type EP3 receptor (K_i for sulprostone, 1.1–4.3 nM). These four EP3 hybrids were expressed at levels similar to that found for the wild-type EP3 receptor (B_{max} = 1503–1920 fmol/mg; Table I). Consistent with the previous reports (16, 25), wild type EP3β showed an ~10-fold higher affinity to [^{3}H]PGE_2 than wild type EP2. In this transient expression system in HEK293 cells, the expression levels of wild type EP3 were also about 1.5-fold higher than wild type EP2.

Agonist-dependent Stimulation of Adenylyl Cyclase by Hybrid EP2-EP3 Receptors—The hybrid receptors showing considerable binding affinities for PGE_2 (EP2-i2, EP2-i2N, EP2-i2C, EP3-i2, EP3-i2N, EP3-i2C, and EP3-i3) were then subjected to cAMP formation analysis. Wild-type mEP2 mediated a butaprost-dependent increase in cAMP. In contrast, the mutant EP2 receptor (EP2-i2) containing the EP3 receptor sequence in the i2 loop almost completely lost the ability to mediate agonist-dependent stimulation of adenylyl cyclase; butaprost failed to elicit a significant increase in cAMP production over the background level (Fig. 1*B*). These results suggested that the i2 loop of EP2 might be essential for G_s coupling. On the other hand, substitution of the i3 loop of the EP3 receptor with the EP2 receptor resulted in a mutant receptor (EP3-i3) that was similar to the wild type EP3β receptor and lacked the ability to mediate stimulation of adelylyl cyclase. However, the mutant EP3 receptor (EP3-i2) in which the i2 loop was replaced with the corresponding EP2 receptor sequence gained the ability to stimulate cAMP production with high efficacy (9.8 ± 0.91 pmol/well) and high sulprostone potency (EC_{50} = 21 ± 1.9 nM) (Fig. 1*C*). Furthermore, a mutant EP2 receptor (EP2-i2C) in which the C-terminal half region of the i2 loop was replaced with the corresponding EP3 receptor sequence was able to stimulate cAMP formation in a fashion similar to the wild-type EP2 receptor. In contrast, a mutant EP2 receptor (EP2-i2N) containing the EP3 receptor sequence in the N-terminal half of the i2 loop again lost the ability to mediate agonist-dependent stimulation of cAMP accumulation. Consistent with these results, substitution of the C-terminal half region of the i2 loop of the EP3 receptor with the EP2 sequence resulted in a mutant receptor (EP3-i3C) that lacked the ability to mediate stimulation of adenylyl cyclase. However, a mutant EP3 receptor (EP3-i3N) in which the i2N region was replaced with the homologous EP2 receptor sequence gained the ability to stimulate cAMP production with high sulprostone potency (EC_{50} = 23 ± 2.1 nM) and high efficacy (22.3 ± 1.9 pmol of cAMP/well). It should be noted that the maximal response by EP3-i2N was significantly higher than EP3-i2. These results suggested that the N-terminal half of the i2 loop in the EP2 receptor (8 amino acids shown in Fig. 1*C*) is required for G_s coupling, and/or the corresponding region of the EP3 inhibits G_s coupling. From these results, we speculated that the i2N region of the EP2 receptor may contain a key amino acid residue required for selective G_s coupling.

Effects of Point Mutations at Tyr^{143} on G_s Coupling of the EP2 Receptor—Among the 8 amino acids in the i2N region, 3 amino acids were identical between mEP2 and mEP3β, which were candidates for key amino acids (Fig. 2*A*). In addition, the rat EP2 receptor contains an Ala residue at position 138 instead of Ser, indicating that Ser^{138} is less important for G_s coupling. We therefore constructed four mutant receptors with Ala mutations at each of the four candidate positions (EP2-Y136A, EP2-G140A, EP2-Y141A, and EP2-Y143A). Among these mutants, EP2-Y136A showed cAMP formation in an agonist dose-dependent manner similar to wild type EP2, whereas EP2-G140A and EP2-Y141A showed high efficacies of cAMP production similar to that of the wild type receptor, although they showed rightward shifted butaprost dose-response curves. In contrast, EP2-Y143A failed to increase cAMP formation above background levels (Fig. 2*B*). The binding properties of EP2-Y143A was similar to those of the wild-type receptor (Table I), suggesting that loss of cAMP producing activity is due to a loss of G_s coupling and that Tyr^{143} in EP2

sequences within the i2 loop of mEP2 and its hybrid receptors (*B*) and those of mEP3β and its hybrid receptors (*C*) are shown *above* the *graphs*. The EP3-derived sequences are *boxed*, and amino acids common in mEP2 and mEP3β receptors are presented in *boldface letters*. The cAMP contents were determined as described under "Experimental Procedures." The results shown are the means ± S.E. of triplicate determinations. *, $p < 0.005$ *versus* pcDNA3; #, $p < 0.005$ *versus* EP3-i2 (EP3-i2N).

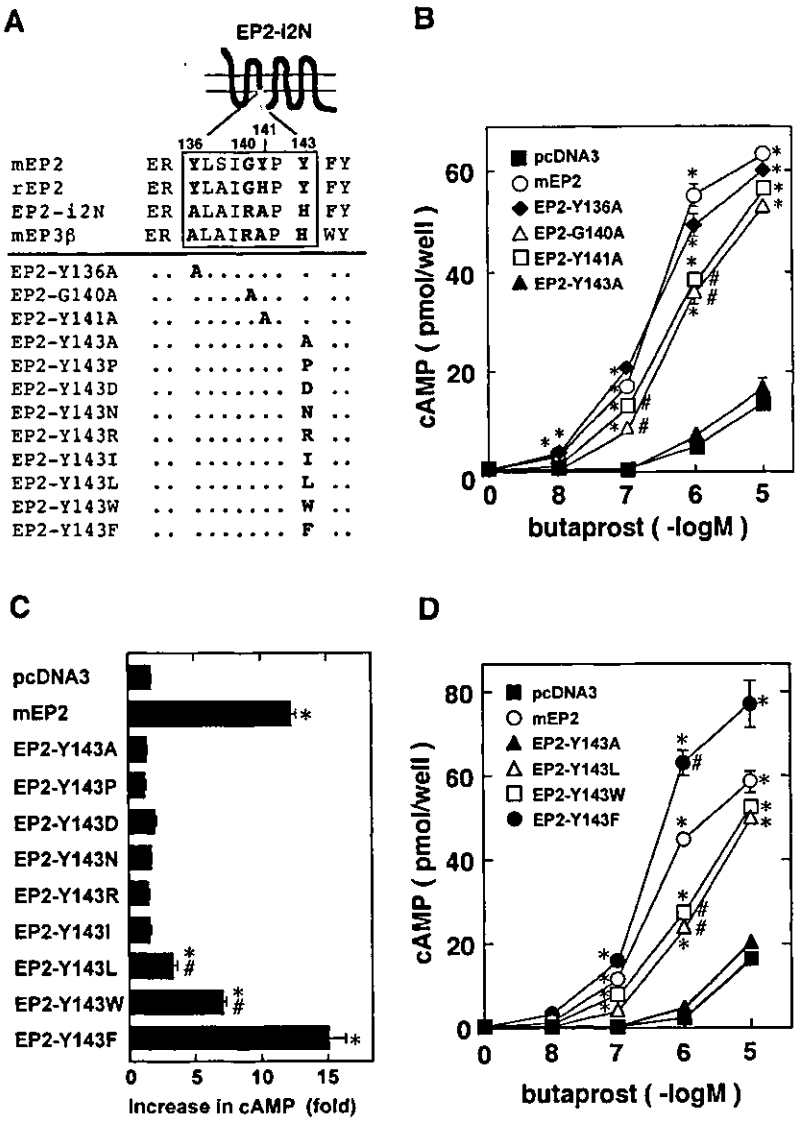

FIG. 2. **Effects of point mutations in the i2 loop on agonist-dependent cAMP formation of mEP2 receptors.** *A*, structures of single amino acid-mutated EP2 receptors. *B*, butaprost dose-dependent cAMP accumulation. HEK293 cells (2×10^5 cells/well) were treated with different concentrations of butaprost, and cAMP production was measured in cells expressing mEP2 and EP2 with point mutations at different positions. *C*, effects of substitutions of Tyr^{143} with various kinds of amino acids in the mEP2 receptor on butaprost-induced cAMP formation. HEK293 cells (2×10^5 cells/well) were treated with 0.1 μM butaprost, and cAMP production was measured in cells expressing mEP2 and EP2 point mutants at Tyr^{143}. The resulting increases in cAMP levels (-fold increase above basal) were determined. *D*, butaprost dose-dependent cAMP accumulation in EP2 with point mutations at Tyr^{143}. The cAMP contents were determined as described under "Experimental Procedures." The results shown are the means ± S.E. of triplicate determinations. *, $p < 0.005$ *versus* pcDNA3; #, $p < 0.005$ *versus* mEP2.

plays a critical role for G_s coupling. We further examined the effects of various amino acid substitutions of Tyr^{143} of EP2 on agonist-induced cAMP accumulation. All mutant EP2 receptors with single amino acid substitutions showed binding properties similar to the wild-type EP2 receptor (Table I and data not shown). Substitution of Tyr^{143} with Phe (EP2-Y143F) resulted in a receptor stimulating cAMP production with an efficiency higher than that of the wild-type EP2 receptor (Fig. 2*D*). Agonist-dependent cAMP accumulation was observed in EP2-Y143W and EP2-Y143L, but their agonist dose dependence was lower than that of the wild type EP2 receptor. Substitution with other residues resulted in a great loss in the ability to stimulate the cAMP response (Fig. 2*C*). The potency order of mutants in butaprost-induced cAMP producing ability was as follows: EP2-Y143F > wild type > EP2-Y143W, EP2-Y143L ≫ EP2-Y143N, EP2-Y143D, EP2-Y143R, EP2-Y143P, EP2-Y143I, EP2-Y143A = 0. These results suggested that the aromatic ring nature of tyrosine at this position in the EP2 receptor appears to be required for G_s coupling with high efficiency.

Substitution of His^{140} with an Uncharged Aromatic Residue Is Sufficient to Confer G_s Coupling on the EP3 Receptor—In order to explore whether a single or a few amino acid mutations can confer G_s coupling on mEP3β, we constructed three mutant EP3 receptors, EP3-H140Y, EP3-R137G/H140Y, and EP3-A133Y/H140Y, all of which include conversion of His^{140} into Tyr (Fig. 3*A*). Surprisingly, all three mutant EP3 receptors exerted sulprostone-dependent cAMP formation in a fashion similar to that of the mutant EP3-i2N receptor (Fig. 3*B*). This finding indicated that the single amino acid substitution of His^{140} into Tyr is sufficient to confer G_s coupling on EP3β. We further constructed mutant EP3 receptors with His^{140} replaced with various amino acids (Fig. 3*A*). All mutant EP3 receptors with single amino acid substitutions showed [^{3}H]PGE_2 binding properties similar to the wild-type EP3 receptor (Table I and data not shown). Substitution of His^{140} with Phe resulted in a mutant EP3 receptor (EP3-H140F) with the most potent ability to stimulate cAMP production; its maximal cAMP production was 2-fold that of the EP3-H140Y receptor (Fig. 3*D*). Moreover, the mutant receptors with His^{140} replaced with Trp and Leu (EP3-H140W and EP3-H140L) exerted moderate and slight increases in cAMP accumulation upon sulprostone stimulation, respectively. The EC_{50} values for sulprostone of these four mutant receptors were similar (~8.5–20 nM). In contrast, the mutant EP3 receptors with substitution of His^{140} into other amino acids elicited no significant increase in cAMP levels (Fig. 3*C*). The potency order of mutants for sulprostone-induced cAMP-producing activity was as follows; EP3-H140F > EP3-H140Y > EP3-H140W > EP3-H140L ≫ EP3-H140D, EP3-

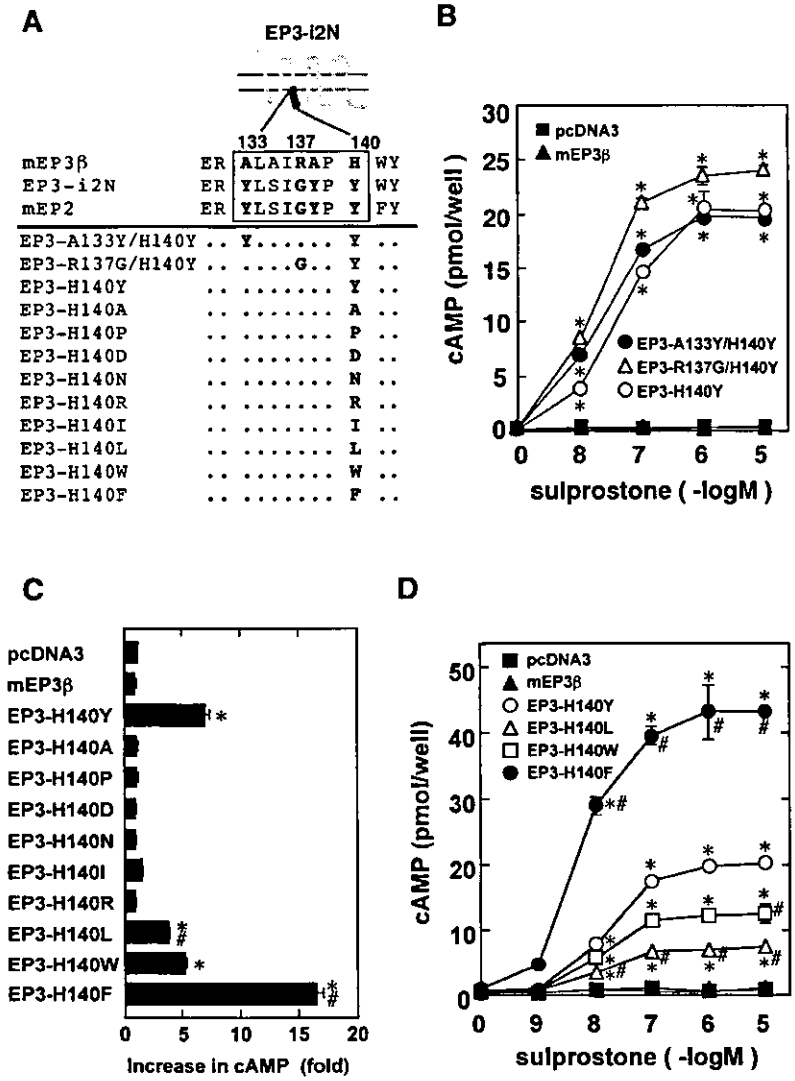

FIG. 3. **Effects of mutations in the i2 loop on agonist-induced cAMP production of mEP3β receptors.** *A*, structures of single or double amino acid-mutated EP3 receptors. *B*, sulprostone dose-response of cAMP accumulation. HEK293 cells (2×10^5 cells/well) were treated with the indicated concentrations of sulprostone, and cAMP production was measured in mEP3β and mutant EP3 receptors. *C*, effects of substitutions of His^{140} with various kinds of amino acids in the mEP3β receptor on sulprostone-induced cAMP formation. HEK293 cells (2×10^5 cells/well) were treated with 10 nM sulprostone, and cAMP production was measured in cells expressing mEP3β and mutant EP3 receptors. The resulting increases in cAMP levels (-fold increase above basal) were determined. *D*, sulprostone dose-dependent cAMP formation in EP3 with point mutations at His^{140}. HEK293 cells were treated with the indicated concentrations of sulprostone, and cAMP production was measured in cells expressing mEP3β and mutant EP3 receptors. The cAMP contents were determined as described under "Experimental Procedures." The results shown are the means ± S.E. of triplicate determinations. *, $p < 0.005$ *versus* pcDNA3; #, $p < 0.005$ *versus* EP3-H140Y.

H140N, EP3-H140R, EP3-H140A, EP3-H140P, EP3-H140I, wild-type mEP3β = 0. The binding affinities of EP3 mutants for PGE_2 and sulprostone were similar to that of the wild-type receptor (Table I and data not shown), suggesting that the difference in the cAMP response was not caused by an altered binding affinity for the agonist. These results indicate that substitution of His^{140} into a noncharged aromatic residue is sufficient to confer G_s coupling on the EP3 receptor. Moreover, the preference of aromatic residues in the efficiency of G_s coupling at the equivalent positions in both EP3 and EP2 receptors suggested that this amino acid contributes to G_s coupling in similar mechanisms for both EP2 and EP3 receptors.

A Cluster of Aromatic Residues at the Center of the i2 Loop Is Required for Efficient G_s Coupling—The present study suggested that the bulky aromatic amino acid at the center of the i2 loop may be one of determinants for G_s coupling in prostanoid receptors. However, when we examined the sequences of the i2 loop of the prostanoid receptors, we found that the EP2 receptor has two more aromatic amino acids, Phe^{144} and Tyr^{145}, just after Tyr^{143}. The existence of three aromatic amino acids at this position is conserved among all members of G_s-coupled prostanoid receptors. Interestingly, the EP3 receptors of various species also contain the latter two aromatic residues, Trp^{141} and Tyr^{142}, just after the key position, His^{140} (Fig. 4). As shown above (Fig. 1, *B* and *C*), interchanging the i2C regions had little effect on the ability of the EP2 and EP3 receptors to stimulate adenylyl cyclase activity, suggesting less importance of the i2C region for G_s coupling. However, this interchange did not alter the existence of the latter two aromatic residues in the cluster. We therefore hypothesized that the latter two residues in the cluster may have potential roles in G_s coupling in the prostanoid receptors, and we examined the effects of mutations at both or either aromatic residues in the EP2 and G_s coupling-acquired EP3 receptors (Fig. 5). In the EP2 receptor, simultaneous alanine mutations of Phe^{144} and Tyr^{145} (EP2-YAA) led to a great reduction in the efficiency of agonist-induced cAMP production. A single alanine mutation at Phe^{144} (EP2-YAY) resulted in a significant reduction of the butaprost-dependent cAMP response, whereas mutation of Tyr^{145} to Ala (EP2-YFA) led to a slight increase in the efficiency of the agonist-induced cAMP response. The rank order of cAMP-producing activity (at 10^{-6} M) of these mutants was as follows: EP2-YFA > mEP2 (YFY) > EP2-YAY ≫ EP2-YAA > EP2-Y143A (AFY) = 0. These results suggest that Tyr^{143} is the most critical for G_s coupling, but Phe^{144} is also required for highly efficient coupling, and Tyr^{145} contributes to G_s coupling only when an aromatic residue is not present at position 144. We investigated whether a similar tendency could be observed in the G_s-acquired EP3 mutant. As discussed above, EP3-H140Y (YWY), which has a cluster of three aromatic residues at the center of the i2 loop, exhibited agonist-dependent adenylyl

Prostanoid receptors		i2N	i2C	
EP2	mouse	ERYLSIGYP	YFY	RRHLSRR Gs
	rat	ERYLAIGHP	YFY	RRRVSRR
	rabbit	ERYLSIGHP	YFY	QCRITRR
	dog	ERYLSIGRP	YFY	QRHVTRR
	human	ERYLSIGHP	YFY	QRRVSAS
EP4	mouse	ERYLAINHA	YFY	SHYVDKR Gs
	rat	ERYLAINHA	YFY	SHYVDKR
	rabbit	ERYLAINHA	YFY	SHYVDKR
	dog	ERYLAINHA	YFY	SHYVDKR
	human	ERYLAINHA	YFY	SHYVDKR
DP	mouse	ECWLSLGHP	FFY	QRHVTLR Gs
	rat	ECWLSLGHP	FFY	QRHITAR
	human	ECWLSLGHP	FFY	RRHITLR
IP	mouse	ERCLALSHP	YLY	AQLDGPR Gs,Gq
	rat	ERCLALSHP	YLY	AQLDGPR
	human	ERCLALSHP	YLY	AQLDGPR
EP3	mouse	ERALAIRAP	HWY	ASHMKTR Gi
	rat	ERALAIRAP	HWY	ASHMKTR
	rabbit	ERALAIRAP	HWY	ASHMKTR
	pig	ERALAIRAP	HWY	SSHMKTS
	bovine	ERALATRAP	HWY	SSHMKTS
	human	ERALAIRAP	HWY	ASHMKTR
EP1	mouse	ERCVGVTQP	LIH	AARVSVA Gq
	rat	ERCVGVTQP	LIH	AARVSVA
	human	ERCVGVTRP	LLH	AARVSVA
FP	mouse	ERCIGVTNP	IFH	STKITSK Gq
	rat	ERCIGVTNP	LFH	STKITSK
	ovine	ERCIGVTKP	IFH	STKITTK
	bovine	ERCIGVTKP	IFH	STKITTK
	human	ERCIGVTKP	IFH	STKITSK
TP	mouse	ERFVGITRP	FSR	PTATSRR Gq,Gi
	human	ERYLGITRP	FSR	PAVASQR

GPCRs with a hydrophobic amino acid		i2N	i2C	
hβ2-AR		DRYFAITSP	FKY	QSLLT Gs
hD1-R		DRYWAISSP	FRY	ERKMT Gs
hH2-R		DRYCAVMDP	LRY	PVLVT Gs
hM2-R		DRYFCVTKP	LTY	PVKRT Gi
hD2-R		DRYTAVAMP	MLY	NTRYT Gi
hA1-R		DRYLRVKIP	LRY	KMVVT Gi
hM1-R		DRYFSVTRP	LSY	RAKRT Gq
hM3-R		DRYFSITRP	LTY	RAKRT Gq
hSP-R		DRYMAIIHP	LQP	RLSAT Gq
hRhod		ERYVVVCKP	MSN	FRFGE Gt

GPCRs with a non-hydrophobic amino acid				
hEDG2		ERYITMLKM	KLH	NGSNN Gi
hEDG3		ERHLTMIKM	RPY	DANKR Gi,Gq,G12
hCXCR4		DRYLAIVHA	TNS	QRPRK Gi
hCXCR6		DRFIVVVKA	TKA	YNQQA Gi

FIG. 4. **Amino acid sequence alignment of the i2 loop of prostanoid receptors and other GPCRs.** The class of G protein to which each receptor can couple is indicated to the *right*. Note that His^{140} is conserved among the EP3 receptors from various species. The amino acids equivalent to Tyr^{143} of EP2 are *boxed*. Among the prostanoid receptors, EP3 and G_s-coupled receptors have bulky hydrophobic residues at the boxed positions (*boxed*). Uncharged aromatic and leucine residues (Phe, Tyr, Trp, and Leu) are indicated in *boldface type*.

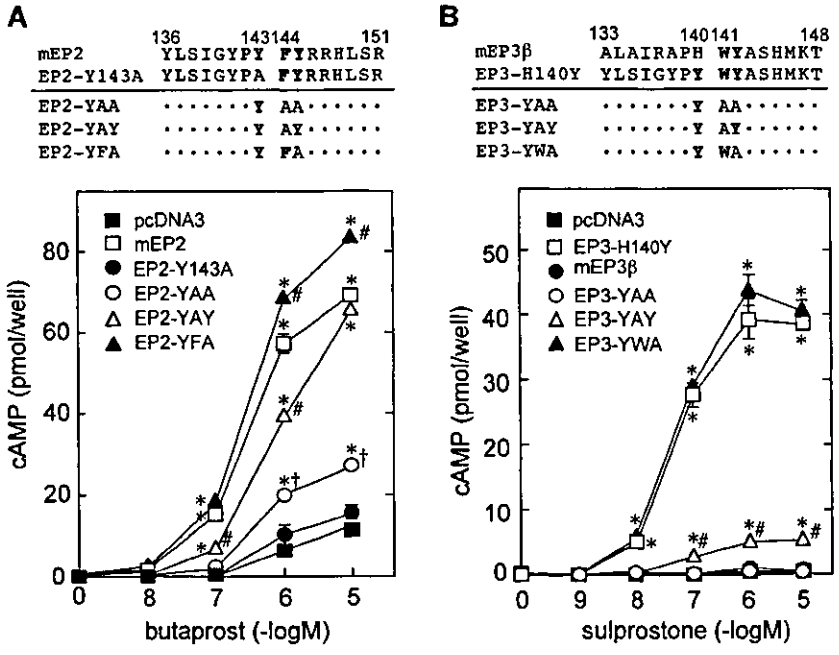

FIG. 5. **Effects of mutations at the amino acids following Tyr^{143} (mEP2) or Tyr^{140} (EP3-H140Y) in the i2 loop on agonist-induced G_s activity of mEP2 and EP3-H140Y receptors.** *A*, butaprost dose response of cAMP accumulation in cells expressing wild type and mutant EP2 receptors. HEK293 cells (2×10^5 cells/well) were treated with the indicated concentrations of butaprost, and cAMP production was measured in cells expressing mEP2 and mutant EP2 receptors. *B*, sulprostone dose-response of cAMP accumulation in cells expressing wild type and mutant EP3 receptors. HEK293 cells (2×10^5 cells/well) were treated with the indicated concentrations of sulprostone, and cAMP production was measured in cells expressing mEP3β and mutant EP3 receptors. Amino acid sequences within the i2 loop of the wild type and mutant EP2 receptors (*A*), and those of the wild type and mutant EP3 receptors (*B*) are shown *above* the *graphs*. The cAMP contents were determined as described under "Experimental Procedures." The results shown are the means ± S.E. of triplicate determinations. *, $p < 0.005$ *versus* pcDNA3; #, $p < 0.005$ *versus* mEP2 (EP2-YFA and EP2-YAY) or EP3-H140Y (EP3-YAY); †, $p < 0.005$ *versus* EP2-YAY (EP2-YAA).

cyclase activity, whereas wild type EP3β (HWY) showed no response upon sulprostone treatment. Simultaneous introduction of Ala residues at positions Trp^{141} and Tyr^{142} led to a complete loss of the ability to stimulate cAMP formation (EP3-YAA). A single alanine mutation at Trp^{141} (EP3-YAY) resulted in a receptor almost unable to stimulate cAMP production, whereas mutation of Tyr^{142} to Ala left agonist-dependent cAMP levels unaffected (EP3-YWA). The rank order of these mutants in cAMP-producing activity was as follows: EP3-YWA = EP3-H140Y (YWY) ≫ EP3-YAY > EP3-YAA, mEP3β (HWY) = 0. Thus, similar results were obtained for the EP3 point mutants, indicating that the existence of a hydrophobic aromatic residue at position 140 is the most critical, but Trp^{141} and Tyr^{142} also contribute significantly and little to G_s coupling, respectively. These results suggest that a cluster of aromatic residues at the center of the i2 loop plays a key role in high efficiency G_s coupling of the prostanoid receptors.

A Gain-of-function Mutation Does Not Alter Intrinsic G_i Activity of the EP3 Receptor—In this study, we used the mEP3β receptor as a prostanoid receptor that does not couple to stimulation of adenylyl cyclase and found that the point mutation at His^{140} is sufficient to confer G_s coupling on the EP3 receptor.

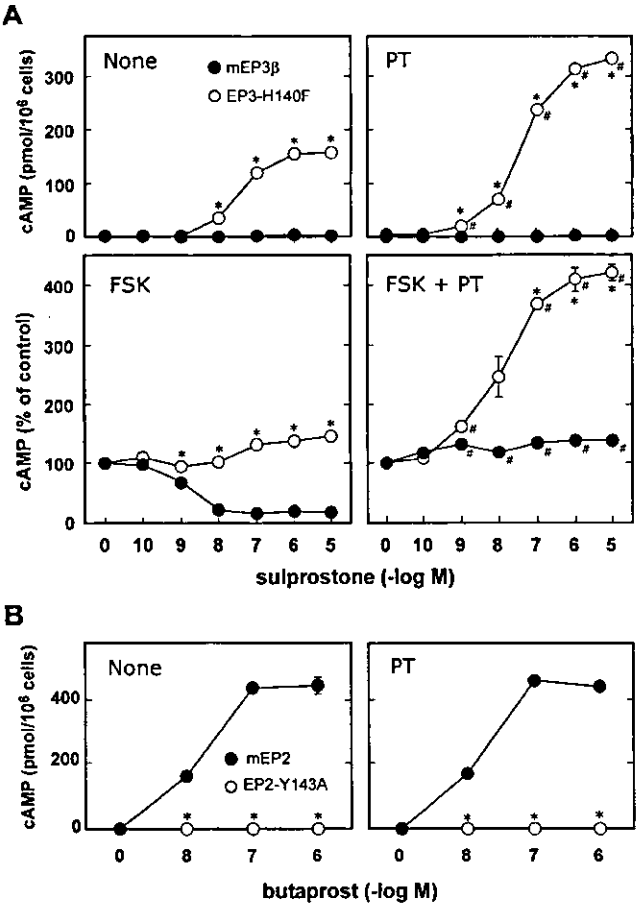

FIG. 6. **Pertussis toxin treatment augmented agonist-induced cAMP accumulation in CHO cells expressing the EP3-H140F but not in CHO cells expressing EP2-Y143A receptor.** *A*, CHO cells expressing mEP3β or EP3-H140F (4×10^5 cells) were pretreated with or without pertussis toxin (*PT*; 20 ng/ml) for 7 h. The cells were then incubated at 37 °C for 10 min with the indicated concentrations of sulprostone in the absence or presence of 10 μM forskolin (*FSK*). *B*, CHO cells expressing mEP2 or EP2-Y143A (4×10^5 cells) were pretreated with or without pertussis toxin and incubated at 37 °C for 10 min with the indicated concentrations of butaprost. The cAMP contents were determined as described under "Experimental Procedures." The results shown are the means ± S.E. of triplicate determinations. *, $p < 0.005$ *versus* wild-type EP3 or EP2 receptor; #, $p < 0.005$ *versus* none (*PT*) or forskolin only (*FSK* + *PT*).

Since the bulky hydrophobic amino acid equivalent to His^{140} of EP3 was proposed to be important in the general interaction with G proteins, we examined whether this point mutation affects intrinsic G_i activity. We established CHO cells stably expressing the G_s coupling-acquired mutant EP3 receptor (CHO-EP3H140F) and compared its functional properties with those of CHO cells expressing wild-type EP3β (CHO-EP3β). As observed in HEK293 cells, the two EP3 receptors showed similar binding affinities (EP3β, K_d = 2.84 nM; EP3H140F, K_d = 3.17 nM), but the expression level of EP3H140F was lower than that of EP3β cells (CHO-EP3β, B_{max} = 1240 fmol/mg; CHO-H140F, B_{max} = 367 fmol/mg). In CHO-EP3β cells, sulprostone did not elicit cAMP formation but inhibited forskolin-induced cAMP formation in a dose-dependent manner with an EC_{50} of 3.1 nM (Fig. 6*A*). This inhibition by sulprostone was completely abolished by pretreatment of the cells with pertussis toxin. In contrast, in CHO-EP3H140F cells, sulprostone dose-dependently stimulated cAMP formation with an EC_{50} of 22 nM, and the compound exhibited no more inhibition against forskolin-induced cAMP production. However, once the cells were pretreated with pertussis toxin, sulprostone-induced cAMP formation was significantly potentiated even in the presence of forskolin. It should be noted that the potentiating effects of pertussis toxin were significantly observed even at 10^{-9} M, suggesting that this mutant receptor is capable of G_i coupling with high efficiency. These results indicate that the EP3-H140F receptor still has an intrinsic G_i activity. Thus, we conclude that the H140F point mutation is sufficient to confer G_s coupling with high efficiency on the EP3β receptor without affecting intrinsic G_i coupling. We further established CHO cells stably expressing the wild-type EP2 (CHO-EP2) and EP2-Y143A receptor (CHO-EP2Y143A) and examined the effects of pertussis toxin on cAMP formation. The two cell lines exhibited same order of PGE_2 binding sites, but the CHO-EP2Y143A cells did not show any cAMP responses upon butaprost treatment (Fig. 6*B*). Moreover, pertussis toxin failed to restore butaprost-induced cAMP response, indicating that loss of agonist-induced cAMP-producing activity in EP2-Y143A is not a result of gain of G_i activity.

A Gain of Function Is Independent of the C-terminal Structure of the EP3 Receptor—We previously reported that mouse EP3 isoforms with different C-terminal tails (EP3α, EP3β, and EP3γ) and C-terminal truncated form (T335) differ in their agonist-dependent G_s activity (21). Since these isoforms are different only in C-terminal structure, we previously demonstrated that the C-terminal tail could play a role in G_s coupling of EP3 receptor. Based on this notion, the effects of i2 loop mutations can be explained by modification of the C-terminal function in G_s coupling. To explore this possibility, we examined the effects of H140F mutation on cAMP-producing activity in other EP3 isoforms (Fig. 7). We employed EP3γ and C-terminally truncated T335, both of which increased cAMP levels in an agonist-dependent manner when expressed in CHO cells (21). In our previous report, the G_s activity elicited by EP3γ observed in CHO cells requires more than 10^{-6} M of agonist, and its maximal response is not as high as EP2 or EP4 receptors, and thus the G_s coupling is considered to be less efficient. Indeed, the increase in cAMP formation by wild-type EP3γ or T335 was hard to detect even in the presence of 10^{-5} M of agonist in the current expression system. On the other hand, introduction of H140F mutation into EP3γ or T335 resulted in a receptor showing agonist-dependent cAMP-producing activity with similar EC_{50} values around 10^{-8} M. Moreover, a significant increase in basal cAMP levels in the absence of agonist was observed in both EP3γ-H140F and T335-H140F but not in EP3β-H140F. The increase in basal cAMP levels by the T335-H140F was significantly higher than that by the EP3γ-H140F. Instead, the agonist-dependent increase in cAMP levels in the mutant T335 appeared lower than that in the mutant EP3γ. However, in the current system, we could hardly detect cAMP increases with any significant difference in wild-type EP3γ and T335 even in the presence of 10^{-5} M agonist. These results suggested that the effects of i2 loop mutation on G_s coupling of EP3 are independent of C-terminal structure, which is likely to govern the balance of constitutive and agonist-induced G protein activation as observed in the G_i activity of the EP3 isoforms.

DISCUSSION

One of the most important findings in this study is the "gain of function" of G_s activity of the EP3 receptor by a point mutation; conversion of the amino acid His^{140} at the center of the i2 loop into an uncharged aromatic residue is sufficient to confer G_s coupling with high efficiency on the EP3 receptor (Fig. 3). The importance of the aromatic moiety of the equivalent amino acid was also demonstrated in G_s coupling of the EP2 receptor (Fig. 2). Previously, the importance of bulky hydrophobic amino